STYRELSEN FÖR

VINTERSJÖFARTSFORSKNING

WINTER NAVIGATION RESEARCH BOARD

Research Report No 59

Patrick Eriksson, Jari Haapala, Istvan Heiler, Hanna Leisti, Kaj Riska and Jouni Vainio

SHIPS IN COMPRESSIVE ICE

Description and Operative Forecasting of Compression in an Ice Field

Sjöfartsverket
Finland

Finnish Maritime Administration

Sjöfartsverket
Sverige

Transportstyrelsen

FOREWORD

In its report no 59, the Winter Navigation Research Board presents the results from a project to develop a measure for the compression in an ice cover that would be suitable for shipping – and also delivered to shipping in an operative manner suitable for navigation guidance – are described. The research work included investigation of the action of compressive ice on ships, development of ice dynamics forecasting models, observation of compression onboard an icebreaker and delivery of forecasting to icebreakers.

The Winter Navigation Research Board warmly thanks Mr. Patrick Eriksson, Mr. Jari Haapala, Mr. Istvan Heiler, Ms. Hanna Leisti, Professor Kaj Riska and Mr. Jouni Vainio for this report.

Helsinki

September 2009

Markku Mylly

SHIPS IN COMPRESSIVE ICE

Description and Operative Forecasting of Compression in an Ice Field

Patrick Eriksson, Jari Haapala, Istvan Heiler, Hanna Leisti, Jouni Vainio

The Finnish Institute of Marine Research

Kaj Riska

ILS Oy

Helsinki 15.3.2007

TABLE OF CONTENTS

1 INTRODUCTION

The compression in an ice field is formed when winds and/or currents are pushing the ice field against a boundary like fast ice edge or coastline. When a wind starts acting on an ice field, the ice starts first to drift. When drifting ice meets a boundary, the coverage of ice increases to 100 % and at the same time some rafting and ridge building occurs. When the forces required to form ridges exceed the driving force due to wind (or current), the ice cover stays immobile while stresses exists in the field.

When a ship proceeds in an ice field where there is compression, larger resistance is encountered and, especially if the ship is stopped, large forces are applied on the ship sides. The compressive situation is considered the most hazardous situation for ships operating in first year ice fields. Thus the development of a warning system for ships operating in the Baltic has been deemed worthwhile. The warning system should make forecasts of compression in terms of quantities relevant to seafarers. Further these forecasts should be conveyed to ships well in forehand of the likely compression situation so that the ships might take relevant action.

This report is the first one from a project where the influence of the compression situation is analyzed and an operational ice compression prediction system is developed. Two main questions are to be tackled in any research on operative forecasting of compression for ships in ice. The first one is the analysis of the compressive situation encountered by ships and especially how the ships experience the compression. This is shortly analyzed in Chapter 2.

The other question is the development of relevant parameters describing the compression encountered by ships and obtaining these from the large scale ice dynamics models used to make the forecasts. Here the problem is that the large scale ice dynamics models average the ice conditions in each grid point used in the forecasting calculations – and these grid points represent an area of the order of magnitude of a square nautical mile. As it is not known in detail what kind of conditions ship operators experience as compressive it was decided to collect data from IB Otso by installing the IceCam system onboard to observe the ship channel after the ship. This system is described in Chapter 3 and the analysis of results in Chapter 5.

Before the analysis of observations, however, the theoretical framework for the analysis is described; this is done in Chapter 5.

Finally, the operative environment to make the compression forecasts and send these to ships is described in Chapter 6 – followed by suggestions for future work given in Chapter 7.

2 SHIP IN COMPRESSIVE ICE

2.1 Description of Compression in an Ice Cover

The term compression in an ice cover refers to a situation where wind and/or current exert drag force on ice cover and the ice starts to drift. The exact modeling of forces and ice motion is described later in this report; here a short general description of ice compression – or as this phenomenon is sometimes called – ice under pressure is given.

When wind drag acts on open pack ice, the ice floes start to move. If the ice motion is restricted by an obstacle like a shoreline, the ice cover starts to compact. First all the open water areas close. This is followed by rafting of ice at the contact points between ice floes. The rafting is followed by ridging. When the force required to ridging is larger than the driving forces, the ice drift stops and stresses i.e. compression in the immobile ice cover will be present. From this description it is clear that the maximum forces that can be present in an ice cover are determined by the forces required to create ice ridges. The process of ice drift is sketched in Fig. 1.

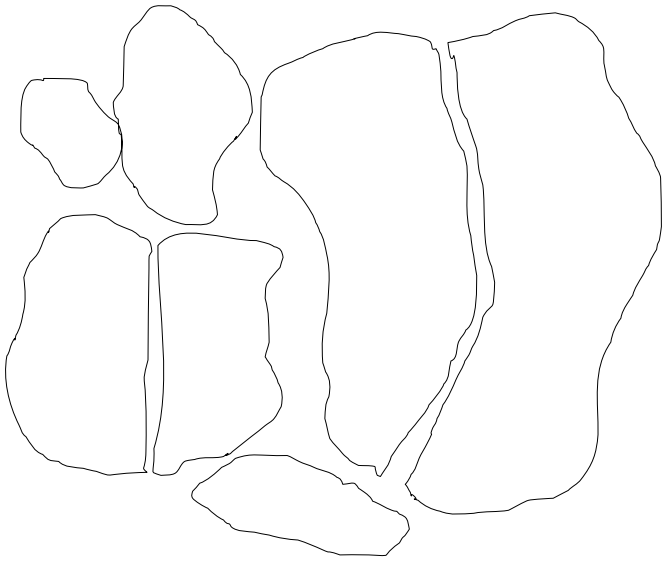

Fig. 1a. The initial pack ice field.

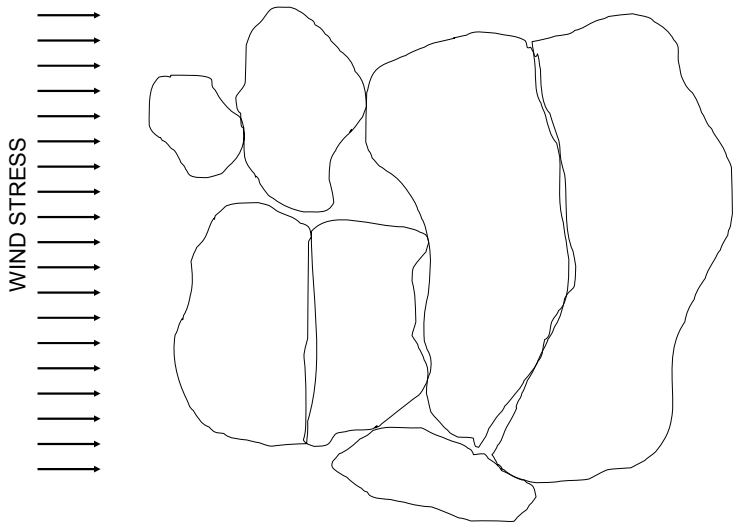

Fig. 1b. Situation when the drift has closed all loose open water areas.

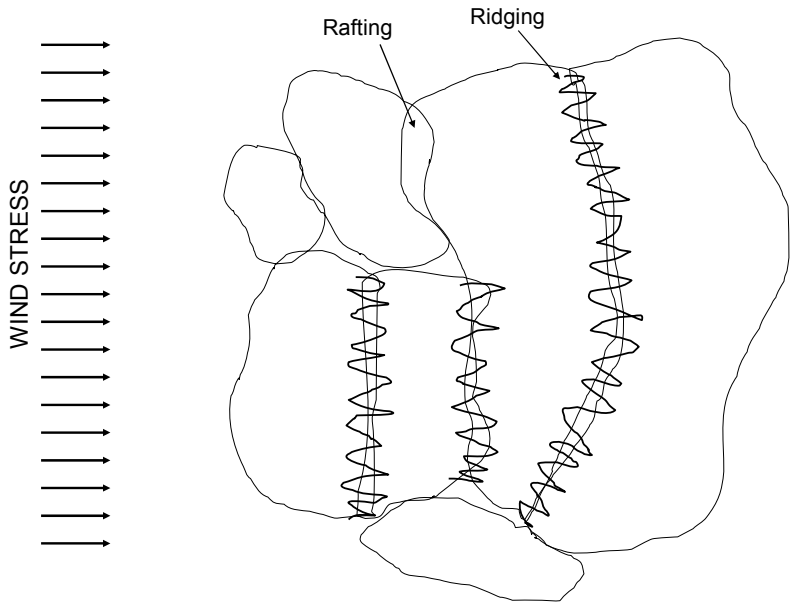

Fig 1c. Situation when the ice drift stops after ridging.

Ice velocities vary from free drift speed of more than 20 cm/s to highly immobile – frozen – conditions. In the Baltic, the main factors causing the ice drift are the wind, currents and internal stresses in the ice pack. Generally, it is known that the internal stress plays a major role when the compactness of the ice pack is high. The effect of internal stress is negligible when the compactness i.e. the coverage is < 0.8 and then the ice velocity is close to the free drift velocity. The free drift of ice is related to the wind speed and direction. The ice drift caused by the wind drag is deviated from the wind direction due to Coriolis force. Zubov (1963) has observed that ice drift is about 28º to the right of the wind direction. Zubov (1963) also observed that the ice drift speed is on average about 2 % of the wind speed (in a free drift situation). These observations corresponds well with the observations made in the Baltic, see Fig. 2. During free drift mode, the pack ice field does not experience any compressive forces.

In the Baltic many observations have been made where the ice pack has been immobile although strong winds have been acting. In these situations the internal stress and resulting compressive forces are very large. The prevailing wind direction (westerly to south-westerly in Gulf of Bothnia) and also the current pattern push ice against the northern shore of the gulf. This creates compressive ice often outside the ports of Oulu and Kemi. This situation is illustrated in Fig. 3.

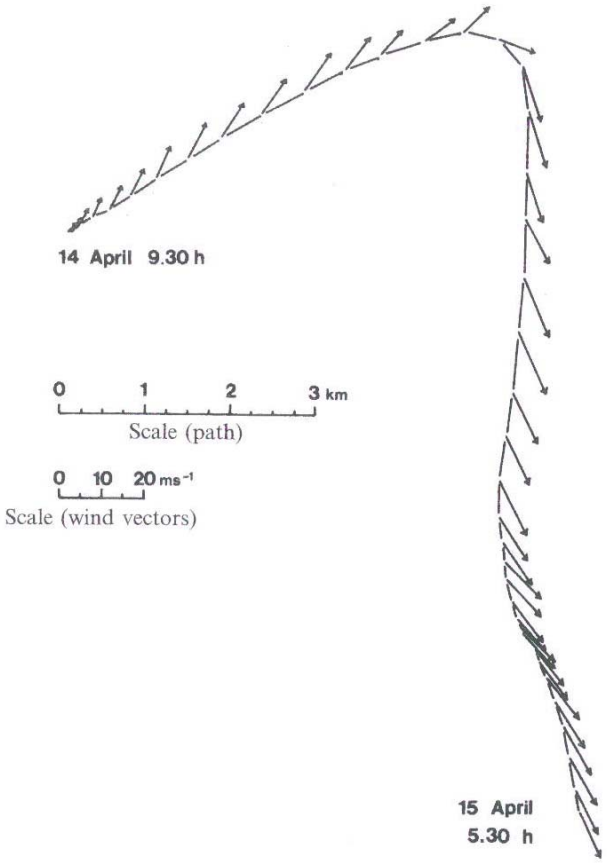

Fig. 2. Observed wind direction and ice drift track. The time interval between the trajectory points is 30 min (Leppäranta 1981).

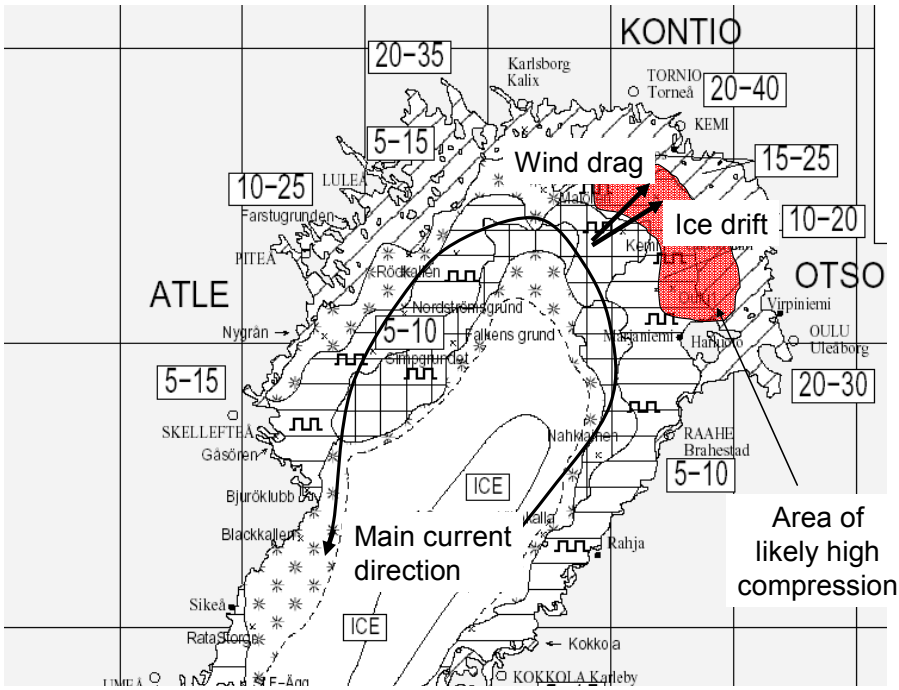

Fig. 3. A typical compressive situation in the Gulf of Bothnia.

2.2 A Ship in Compressive Ice

When a ship is proceeding in compressive ice where the driving force and thus the largest principal stress is normal to the ship track, the channel the ship makes starts to close after the vessel. If the edges of the closing ice sheet touch the sides of the ship, large forces arise and the ship is likely to stop. Fig. 4a shows a vessel that has been stopped in compressive ice in the Baltic and the channel the ship made has closed completely. Similar case observed for icebreaker Sedov in the Arctic waters is described in Zubov (1963), Fig. 4b.

Fig. 4. A ship stuck in compressive ice (photo: Atso Uusiaho).

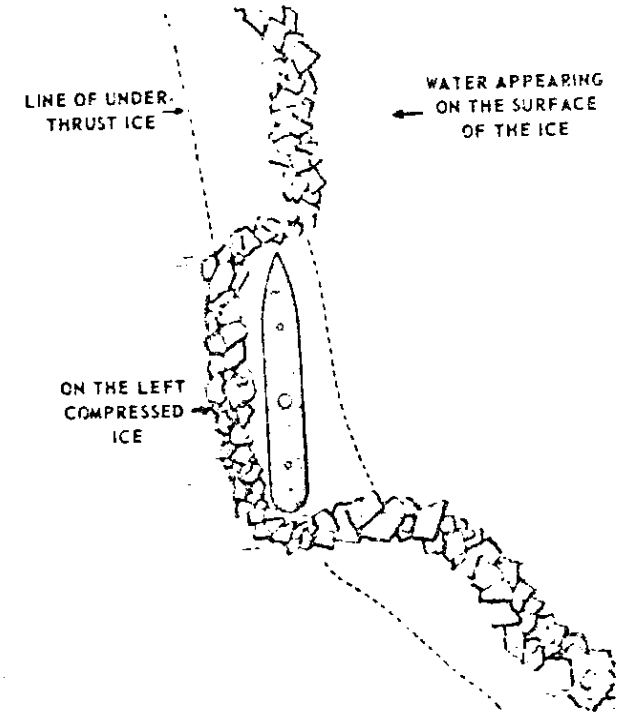

Fig. 4b. Icebreaker Sedov stuck in compressive ice (Zubov 1963).

When a ship proceeds in an ice cover where there is compression, the ice cover initially is at rest but the channel starts to close after the vessel. Sometimes it happens so that the ship passage triggers an ice motion more than just the channel closing. In this case the driving force together with the inertia that the moving ice cover acquires, is enough to develop forces that are higher than the forces required for ridging. This also emphasizes the danger in the hot spots present in closing pack ice where two ice floes are in contact.

The compressive situation is illustrated in Fig. 5. After the ship has opened the channel, it starts to close. If the ship breaks a channel the width of which is B + 2·d, where the ship beam is B and d is the amount the channel is wider than the ship beam and the channel starts to close with speed v_i immediately after it has been broken, then the ice cover moves in time T a distance $s_1 = s_2$ in symmetrical situation. Thus the angle formed by the closing ice is $\arctan(v_i/v_s)$ where v_s is the speed of the ship. This situation is illustrated in Fig. 5.

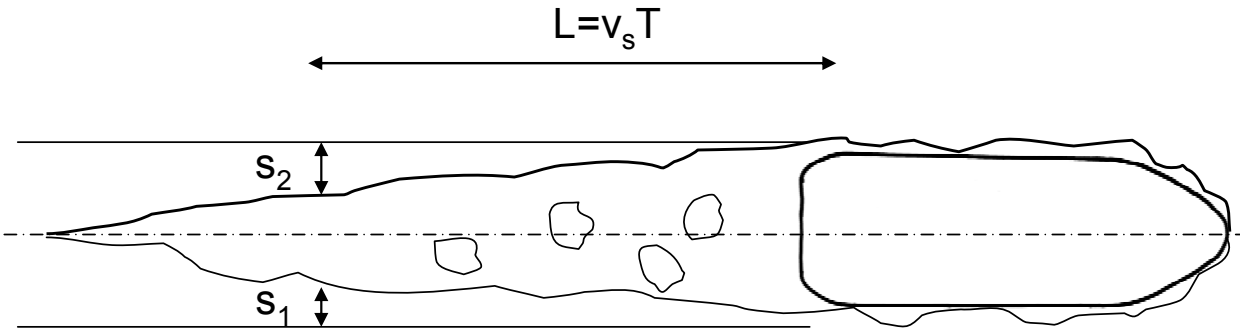

Fig. 5a. The closing channel after the vessel in compressive ice in ship related coordinates.

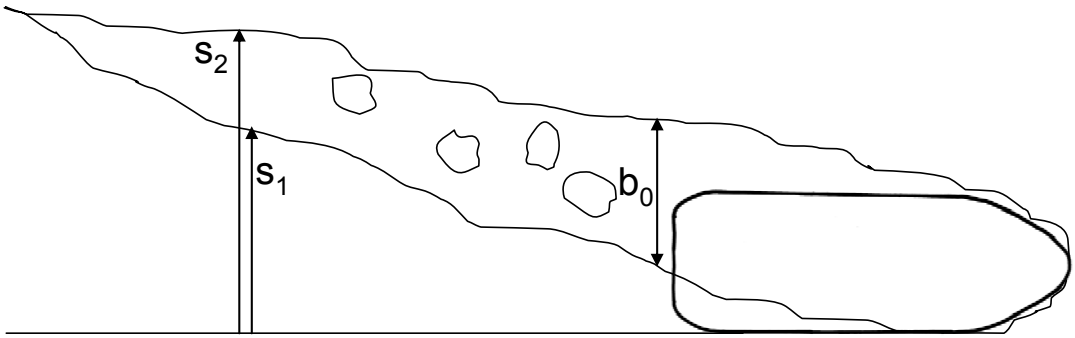

Fig. 5b. The closing channel after the vessel in compressive ice in sea bottom fixed coordinates.

The analysis of the closing speed of the channel can be related to quantities given by ice dynamics calculations. Especially the strain in the ice field and similarly the strain rate can be related to the closing speed of the channel. If the distances s_1 and s_2 are measured in fixed coordinate system, then it can be assumed that the general ice cover motion is $v_i = \dot{s}_2$ and that the closing speed is $\dot{b} = \dot{s}_1 - \dot{s}_2$. The strain is now

$$\varepsilon = \frac{s_1 - s_2}{b_0} \tag{1}$$

and strain rate

$$\dot{\varepsilon} = \frac{\dot{s}_1 - \dot{s}_2}{b_0}. \tag{2}$$

If the ice cover is not moving before the ship passage, then it can be assumed that the ice cover

down-wind or down-current is not moving i.e. $\dot{s}_2 = 0$ (the coordinates can be set so that $s_2 = 0$).

The ratio of the speeds may be such that the edges of the channel touch the parallel midbody of the vessel - in this situation the ice is crushed against the midbody and this gives rise to added resistance. This added resistance is the frictional force arising from the crushing of ice against the midbody, see Fig. 6. If the crushing force is denoted as q, then the frictional force i.e. added resistance per unit length of the ship is

$$q_\mu = \mu \cdot q \tag{3}$$

where μ is the coefficient of friction. The equation for total resistance in a closing channel is

$$R_{iTC} = R_{iT} + 2 \cdot L_C \cdot q_\mu = R_{iT} + 2 \cdot (L_{PAR} - \frac{v_S}{v_i} \cdot d) \cdot q_\mu, \tag{4}$$

where R_{iTC} is the total resistance in compressive ice, R_{iT} total resistance in similar ice without compression and L_{PAR} the length of the ship's parallel midbody (other quantities are explained in Fig. 3). It should be noted here that the extra width (above the ship beam) of the channel, d, might be a function of ship speed as the ice floe size broken by bending is a function of speed

.

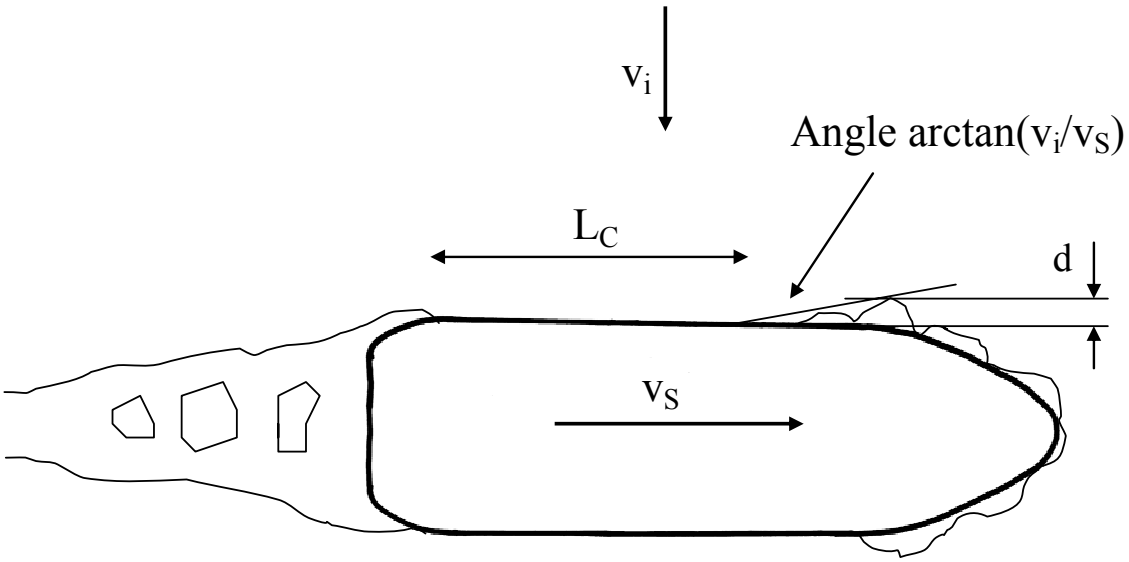

Fig. 6. A ship in compressive ice (Riska et al. 2006).

The schematic model of a ship in compressive ice is important because the parameters influencing the ship getting stopped in compressive ice are separated to parameters related to the ship (d, L_C, v_s) and parameters related to the ice field (q, v_i). The force acting on the vessel in a closing channel, q, is a large scale quantity as it is the average force acting on the whole length L_C. Thus it – as well as the channel closing speed v_i, may be obtained from large scale ice dynamics models. The local force acting on the vessel side is, however, much larger than the large scale compressive force. The order of magnitude of the local force is MN/m while the large scale compressive force is of the order of 100 kN/m.

The above analysis suggests that there are three scales that are to be studied in the compression. These scales and the related length scale are the following:

1. Scale of ice dynamics — length scale grid cell width D, here 1 nm
2. Ship performance scale — length scale ship length L
3. Ship loading scale — length relevant to structural elements, ship frame spacing s or longitudinal frame span l.

Several observations have shown that the ice line load i.e. load per unit horizontal width depends

on the length the measurement is done. Fig. 7 depicts some results from ship borne measurements. All these measurements suggest a form of

$$q = C \cdot L^{-0.7}, \ [L] = m \tag{5}$$

for the measurement results. The constant C varies a bit, but for the Baltic the result of maximum ice forces from IB Sisu measurements would be most suitable – here C = 1310 kN/m (when lengths are given in m). This scaling results in ship scale to a value q = 39 kN/m (L = 150 m) and in the scale of ice dynamics 6.8 kN/m. The latter value corresponds to a total force of $1250 \cdot 10^4$ N which compares well with the maximum compression values calculated

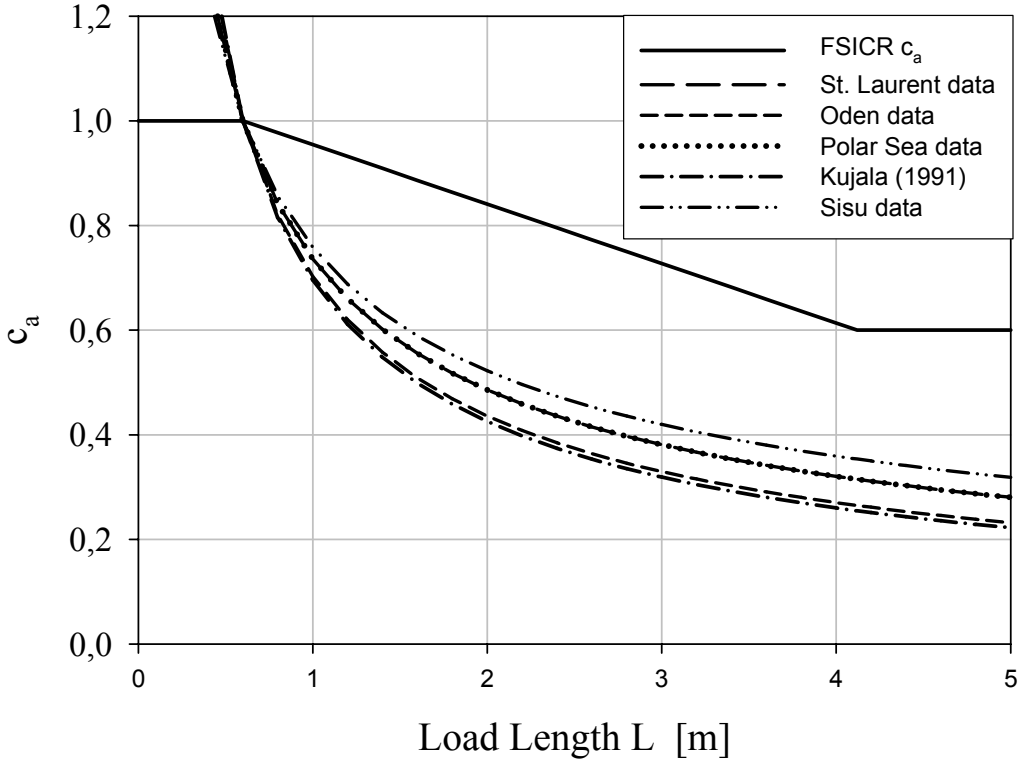

Fig. 7. The dependency of the line load on the contact length in various ship borne measurements scaled so that they all are one when L = 0.6 m.

It was decided that the closing speed of the channel is to be investigated in the present project as it was identified as a parameter that is obtainable from video records – these are described in the next chapter. It would be especially interesting to clarify if the closing speed of the channel is influenced by the ship sailing direction relative to the stress field and thus also relative to the driving force. Further the stress in the ice field is to be investigated with ice dynamics modeling. All these results are then collected together for the observed compression events.

3 ICECAM

3.1 IceCam Instrument on IB Otso

During the winter and spring 2006 an IceCam equipment was installed on the I/B Otso, which operated in the northern Bay of Bothnia. The aim was to test the suitability of a camera apparatus for monitoring sea ice dynamics and deformation and also – if the equipment is suitable – observe the ice motion.

Equipment

The IceCam is a camera based observation unit developed by SAMS (The Scottish Association for Marine Science) and Norwegian Polar Institute, Norway (Hall et. al., 2002). The instrument installed on IB Otso was borrowed from Norwegian Polar Institute for the winter/spring 2006. It was installed onboard IB Otso 2.2.2006 and removed 9.5.2006 and thus it operated in total for 96 days.

The IceCam is a stand-alone system consisting of one camera unit, one data storage unit and an external GPS antenna. The data storage unit had an in-built cluster with power supply, a laptop PC and a GPS receiver. The units were connected with weather-proof cables. The camera itself was an AXIS 205 Network Camera, enclosed in a weather-proof casing. It was tied to the railing on the roof of the port side wing of the bridge, 24 meters above water line. It was installed looking backward so that the images covered the aft deck and the ice field behind the icebreaker. The data storing unit was placed in the mast in a small protected space with heating. The GPS aerial was attached outside the mast. All cables were drawn through a ventilation duct (Figures 8 - 11).

Fig. 8. Installation overview of IceCam on board IB Otso, winter 2006.

Fig. 9. IceCam seen from aft deck.

Fig. 10. Camera unit attachment.

Fig. 11. Camera unit seen from the deck below.

Images

For the images taken by the IceCam to be suitable for the ice pressure study, a short enough interval between shots was required. Therefore IceCam was set to save an image once a minute. Apart from a few gaps in the GPS data, the IceCam system worked according to expectations and for the whole study period this resulted in totally 137436 pictures. The image acquisition was satisfactory, bearing in mind that the light conditions varied a lot. Even in dusk the contrast and distinction of details was gratifying. Only the pictures taken in total darkness are hard to make use of. Four examples of the images are shown in Fig. 12.

02.17.2006 15:30 UTC

02.27.2006 09:27 UTC

02.06.2006 11:13 UTC *02.04.2006 15:46 UTC*

Fig. 12. Examples of Ice Cam images.

Suggestions for Future Application

Even if the IceCam borrowed from Norwegian Polar Institute fulfilled all expectations, a future version of the IceCam would have to be better suited for the demands that arise. To serve the needs of operational work, the system is required to be accessible on-line or with some similar real-time output. This way the imagery would benefit both icebreaker operation and scientific use. To make this possible there would have to be a connection to the ship's data network. Also the bridge crew could benefit from this by getting live video imagery from the camera. Particularly when the icebreaker is assisting or towing a vessel, the scientific benefit from the images is limited. As this is the case for a great part of the time, any usage for other purposes is preferable.

When snapshots are taken with one-minute intervals, the amount of image files rapidly gets immense. Therefore data storage and handling would require a clever application to make all data usage easier.

3.2 Correction of Both Lens and Perspective Distortion in the IceCam Images

Lens distortion

In all the AXIS 205 Network Camera (which is used in the IceCam) images the horizon line is strongly bent, the difference between the vertical location (= row) of the horizon in the middle of the images and at the first/last columns of the images is about 10 pixels. In principle this could be simply due the earth's curvature. However, a photogrammetric computation showed that the earth's curvature does not have any effect in this case; the camera location height (24 m) and horizontal field of view (appr. 48º) are small enough to make the effect of Earth's curvature negligible. Thus, the horizon should be a straight line and in that manner the bending is due to a lens distortion. The barrel distortion is shown in the image below, Fig. 13.

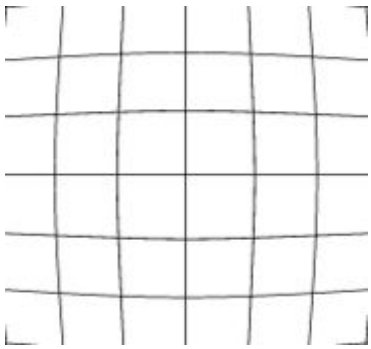

Fig. 13. The barrel distortion.

The computational removal of the barrel distortion was performed by using GIMP image manipulation software (wide angle filter is obtainable from the Internet page http://members.ozemail.com.au/~hodsond/gimp.html), in two steps: 1) the control parameters of the filter were adjusted by visual inspection and 2) a GIMP-script was iteratively run inside a Linux-shell to perform the correction for a large set of images. As an example the original image (left) and corrected image are shown in Fig. 14. The correction removes some edge rows and columns to preserve the original row and column count.

Fig. 14. An example of the removal of the barrel effect.

Perspective distortion

The correction of the perspective distortion is essential concerning the question whether the breadth of the channel changes as function of time. The principle of the computational correction of the perspective distortion can be seen from the image below, Fig. 15.

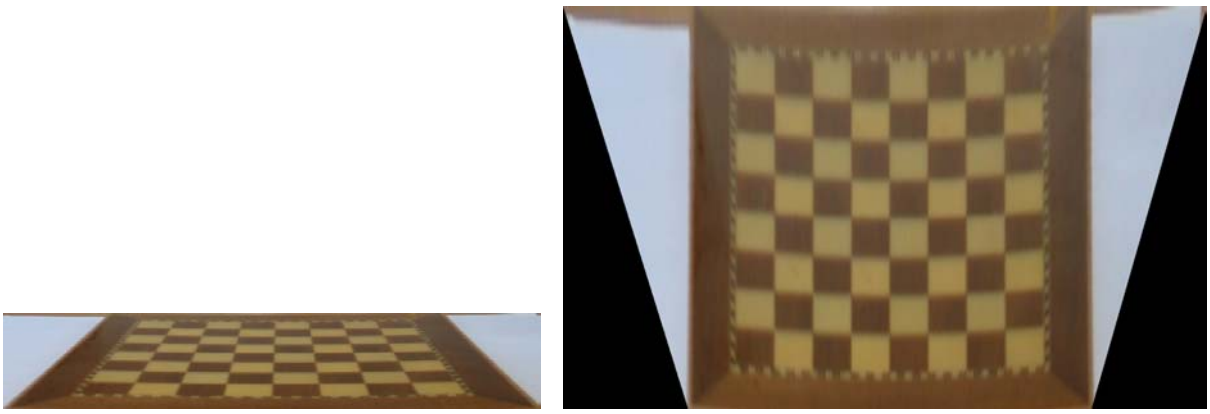

Fig. 15. The correction for the perspective, original image and the corrected one.

For the computation a set of MATLAB-functions were used. These can be obtained from 'http://www.csse.uwa.edu.au/~pk/research/matlabfns' (section 'Functions supporting projective geometry') that were first modified to be of Octave compatibility. The computation requires that the new locations of the image corners are given in respect to the top left corner of the original image (in row/column coordinate system).

It is possible to reproject the pixel corner points back to a (spherical) Earth's surface if the camera orientation and camera parameters (focal length and dimensions of the active image area) are known. In the present case the remaining unknown parameters were the vertical and horizontal tilt angles of the camera. These were approximated by using the other parameters and the location of the horizon. The photogrammetric computation method in question was originally developed at FIMR for purposes of video image based wave analysis; details are omitted here.

As a result the method gives for each pixel corner point the corresponding location (x, y and z-coordinates) on a spherical surface. In this case the correction of the whole images (region below horizon) was not possible due to the lack of enough CPU-resources, hence the correction was performed only to a smaller area in the middle of the images. Also the resulting images were cropped to get smaller file sizes. The resolution (appr. 0.09 m) was selected according to the average pixel size at the bottom of the image (length of the bottom line / image column count).

3.3 Computation of the Channel Widths at Chosen Locations

From the point of view of the (semi)automatic identification of the channel edges, three main cases can be separated. In the first case there exists a clear water zone in the middle of the channel and an ice rubble zone near the channel edges, the second case is a clear water channel and the last case is a channel with no clear water. In the composite image below, some examples of the mentioned cases are presented; red dots indicate the locations of the channel edges. In the first case is also noticeable that the rubbled ice zone becomes more and more blurred as the horizon is approached.

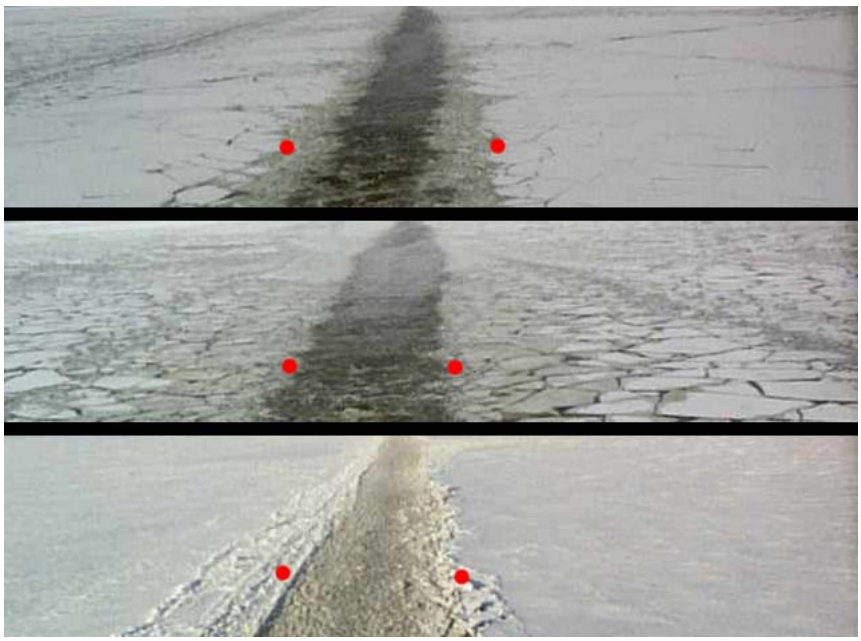

Fig. 16. The identified locations of channel edges from corrected images.

The implemented algorithm to identify the locations of the channel edges (columns of the corrected image) and to compute the channel widths at user given locations (rows of the corrected image) has three steps:

1. Selecting the computation window, rows [r0-100, r0+100] where r0 is the user given row (200 rows corresponds to circa 19m distance). This is necessary to avoid errors due to 'fluctuations' of the channel edge line, see image below.
2. Histogram equalization of the pixel values to increase the contrast and scaling of the equalized pixel values to interval [0,100].
2. Computing horizontal profile from the window as column means and smoothing of the profile line.
4. Determination of the channel edges by thresholding; selecting the section of the profile where values remain under the threshold value.

Example of the 'fluctuations' of the channel edge lines due to the positioning of ice blocks, comparison of channel widths at single rows would give non existing compression cases.

Fig. 17. An example of the fluctuation of the identified channel edge.

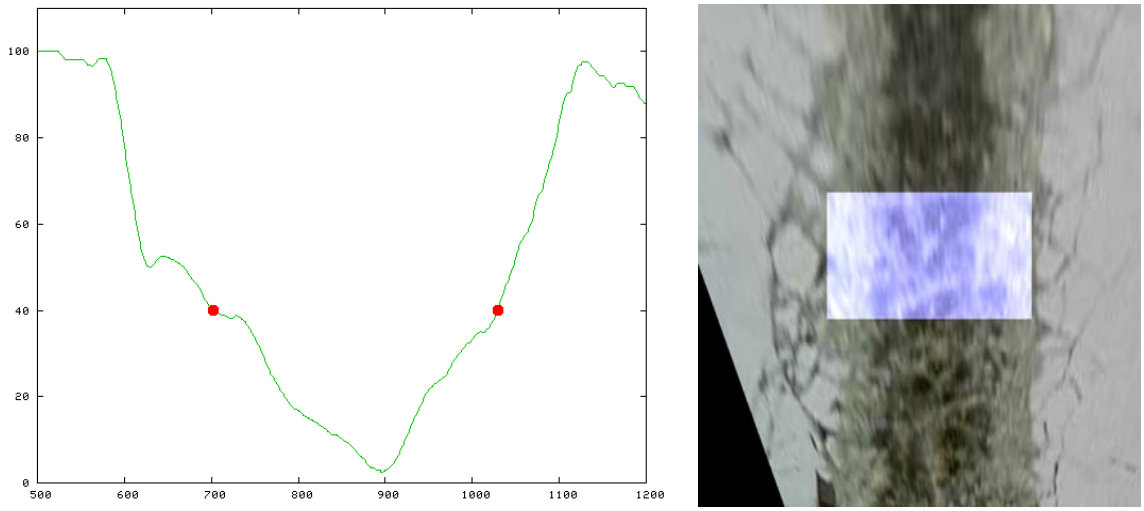

Fig. 18. Example of the horizontal profile (channel edges as red dots) and the location of the channel section in the rectified image.

4 MODELLING OF ICE COMPRESSION

Ice compression forecast are made with the operation sea-ice model of the FIMR. The model provides forecast of ice motion, concentration, thickness, ridges and deformations for the Baltic Sea. The operational model is a multicategory sea-ice model developed originally for the climate research (Haapala et al., 2005). The model physics and numerics are same both in operational and climate simulations. The only differences are in the horizontal resolution and atmospheric forcing used. The model resolves ice thickness distribution, i.e. ice concentrations of variable thickness categories, redistribution of ice categories due to deformations, thermodynamics of sea-ice, horizontal components of ice velocity and internal stress of the ice pack. Presently, no assimilation is used for the model predictions.

Horizontal resolution of the model is 1 nm. The sea ice forecast out to 54 hours are made once a day. Sea ice model is forced by the HIRLAM forecast. Initial SST is obtained from the ice charts. The model produce forecast of the following variables:

total sea ice concentration
undeformed ice thickness
rafted ice mean thickness and concentration
ridged ice mean thickness and concentration
ridge height
ice velocity
ice compression

The compression **F** is defined as the force due to internal ice interaction. The **F** is resolved together with ice motion are determined by the momentum balance equation, which reads,

$$m(\frac{D\vec{u}}{Dl} + f\hat{k} \times \vec{u}) = A(\vec{\tau}^{\,a} + \vec{\tau}^{\,w}) - mg\nabla H + F \tag{6}$$

where m is the total ice and snow mass, $\vec{u}$ is the horizontal ice velocity vector, f is the coriolis parameter, $\hat{k}$ is the upward unit vector, $\vec{\tau}^{\,a}$ is the air stress vector, $\vec{\tau}^{\,w}$ is the water stress vector, g is the gravitational acceleration, ∇H is the sea surface tilt and **F** is the internal friction of ice.

The ice compression or internal friction is

$$\mathbf{F} = \nabla \cdot \sigma \tag{7}$$

where σ is the internal stress tensor is

$$\sigma = \begin{pmatrix} \sigma_{xx} & \sigma_{xy} \\ \sigma_{yx} & \sigma_{yy} \end{pmatrix} \tag{8}$$

The diagonal components are compressive or tensile stresses and off-diagonal components are shear stresses. The internal stress of the pack ice is solved according to the viscous-plastic theology with elliptical yield curve (Hibler, 1979).

$$\sigma = 2\eta\dot{\varepsilon} + (\xi - \eta)tr\dot{\varepsilon}I + \frac{1}{2}PI \tag{9}$$

where η is the shear viscosity, ξ is the bulk viscosity, $\dot{\varepsilon}$ is the strain rate tensor, **I** is the unit

tensor and the P is the ice strength.

The ice strength parameter links ice dynamics to ice thickness distribution and in the multi-category model the ice strength parameter P is directly related to the energy consumed during deformation (Rothrock, 1975; Flato and Hibler, 1995)

$$P = C_f C_p \int_0^\infty h^2(\omega_u + \omega_d)dh \tag{10}$$

where the parameter C_f describes the ratio of total energy losses to the potential energy change. $C_p = 0{,}5g(p_i/p_w)(p_w - p_i)$, where p_i and p_w are the densities of ice and water, respectively. C_f has been set to be 17.0 (Flato and Hibler, 1995).

The relationship of the bulk and shear viscosities is defined by following manner (Hibler, 1979)

$$\eta = \frac{\xi}{e^2} \tag{11}$$

$$\xi = 0.5P\left[\left(\dot{\varepsilon}_{xx}^2 + \dot{\varepsilon}_{yy}^2\right)\left(1 + e^{-2}\right) + 4e^{-2}\dot{\varepsilon}_{xy}^2 + 2\dot{\varepsilon}_{xx}\dot{\varepsilon}_{yy}\left(1 - e^{-2}\right)\right]^{-1/2} \tag{12}$$

where e is a constant describing the aspect ratio of the elliptic yield curve ($e = 2$).

Components of the ice compression are

$$\mathrm{F_x} = \left[\nabla \cdot \sigma\right]_\mathrm{x} = \frac{\partial \sigma_{\mathrm{xx}}}{\partial \mathrm{x}} + \frac{\partial \sigma_{\mathrm{yx}}}{\partial \mathrm{y}} \tag{13}$$

$$\mathrm{F_y} = \left[\nabla \cdot \sigma\right]_\mathrm{y} = \frac{\partial \sigma_{\mathrm{xy}}}{\partial \mathrm{x}} + \frac{\partial \sigma_{\mathrm{yy}}}{\partial \mathrm{y}} \tag{14}$$

Substituting (8) to the above equation gives final form for the ice compression equations

$$\mathrm{F_x} = \frac{\partial}{\partial \mathrm{x}}\left[(\eta + \xi)\frac{\partial \mathrm{u}}{\partial \mathrm{x}} + (\xi - \eta)\frac{\partial \mathrm{v}}{\partial \mathrm{y}} - \frac{\mathrm{P}}{2}\right] + \frac{\partial}{\partial \mathrm{y}}\left[\eta\left(\frac{\partial \mathrm{u}}{\partial \mathrm{y}} + \frac{\partial \mathrm{v}}{\partial \mathrm{x}}\right)\right] \tag{15}$$

$$\mathrm{F_y} = \frac{\partial}{\partial \mathrm{y}}\left[(\eta + \xi)\frac{\partial \mathrm{v}}{\partial \mathrm{y}} + (\xi - \eta)\frac{\partial \mathrm{u}}{\partial \mathrm{x}} - \frac{\mathrm{P}}{2}\right] + \frac{\partial}{\partial \mathrm{x}}\left[\eta\left(\frac{\partial \mathrm{u}}{\partial \mathrm{y}} + \frac{\partial \mathrm{v}}{\partial \mathrm{x}}\right)\right] \tag{16}$$

$\mathbf{F_x}$ and $\mathbf{F_y}$ express the ice compression per unit area i.e. its unit is N/m^2. In this case, the unit area is the area of the model grid and multiplicating $\mathbf{F_x}$ and $\mathbf{F_y}$ with the area (1.852 x 1.852 km) yield for an estimate of the large scale compressive ice force. This large scale compressive ice force, which unit is N, is used in the operational ice compression forecast.

An essential but virtually unknown question is the relationship between the large scale compressive force of ice and the forces in the scale of the ship. In principle, if the ice thickness distribution within the model grid cell is know, the large scale compressive force of ice can be downscaled and estimate local forces on the ship sides.

An example of the compression forecast given in terms of force is given in Fig. 19. In these forecasts also the direction of the largest principal stress is shown – this direction is likely to correspond to the course of easiest navigation.

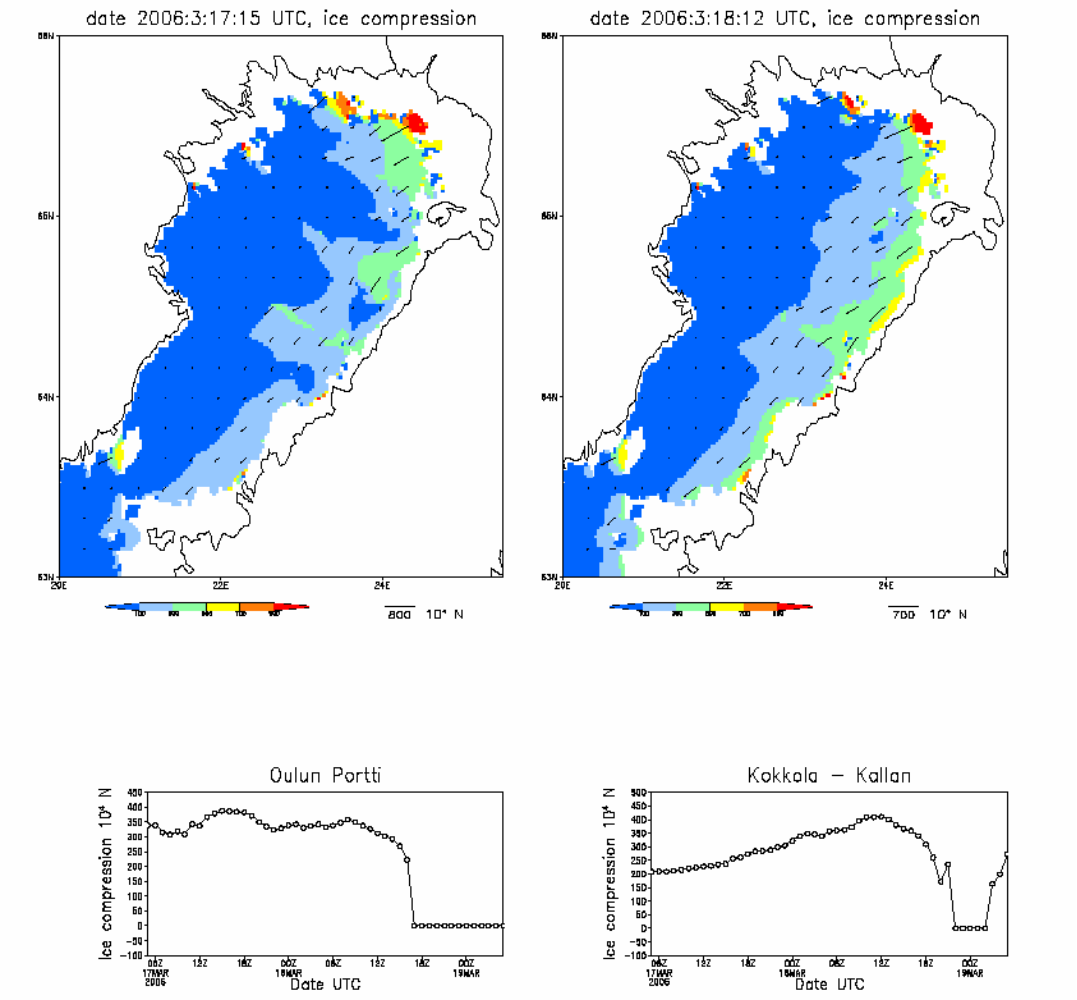

Fig. 19. An example of the compression forecasts in units of force [N].

The physical unit used here for ice compression is not very suitable for the practical applications. Ice compression could be indicated by a simple linear scheme also, like a four category scheme where 0 means no compression, 1 denotes modest compression, 2 for strong compression and 4 indicating severe compression. If the relationship between the modelled compression and actual compression experienced by the ship is known, the modelled ice compression can be scaled to the four category scale. Unfortunately there are not enough systematic observations of the effect of the ice compression on navigation and thus we present here a first order estimate of the scaling (Fig. 20). In this example, the long term simulation data for determining ice compression distribution is used and a quadratic relationship between the modelled and observed ice compression stipulated.

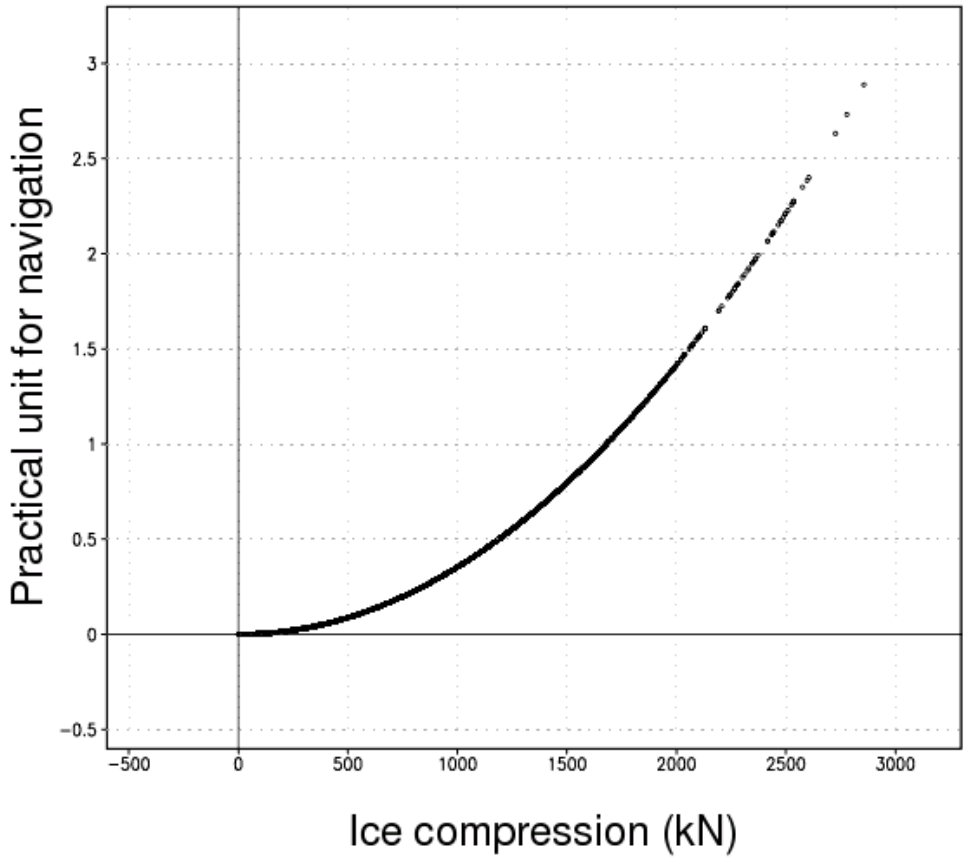

Fig. 20. Illustration of a possible relationship between the modelled ice compression and the scale used for ice compression forecast.

5 ANALYSIS OF OBSERVED COMPRESSION EVENTS

5.1 Ship records

The occurrence of compression is not easy to detect from the IceCam images. Thus the notes made in the IBNet records by the crew of IB Otso were used to identify situations when there was compression in the ice field. This way 9 cases of compression were identified. These are listed in Table 1. The location of the compression points is shown in Fig. 21. Several of these are inside the shorefast ice zone which makes it difficult for the analysis as the forecasting of compression is difficult.

Table 1. The observed compression events

Compression reports from the ship

Case n:r	Date	Position
1	7.2.	inlet to Oulu fairways
2	15.2.	inlet to Oulu fairways
3	17.2.	north of lighthouse Kemi 2
4	8.3.	north of lighthouse Kemi 2
5	10.3.	lighthouse Kemi 1
6	30.3.	inlet to Oulu fairways
7	8.4.	inlet to Oulu fairways
8	26.4.	lighthouse Kemi 1

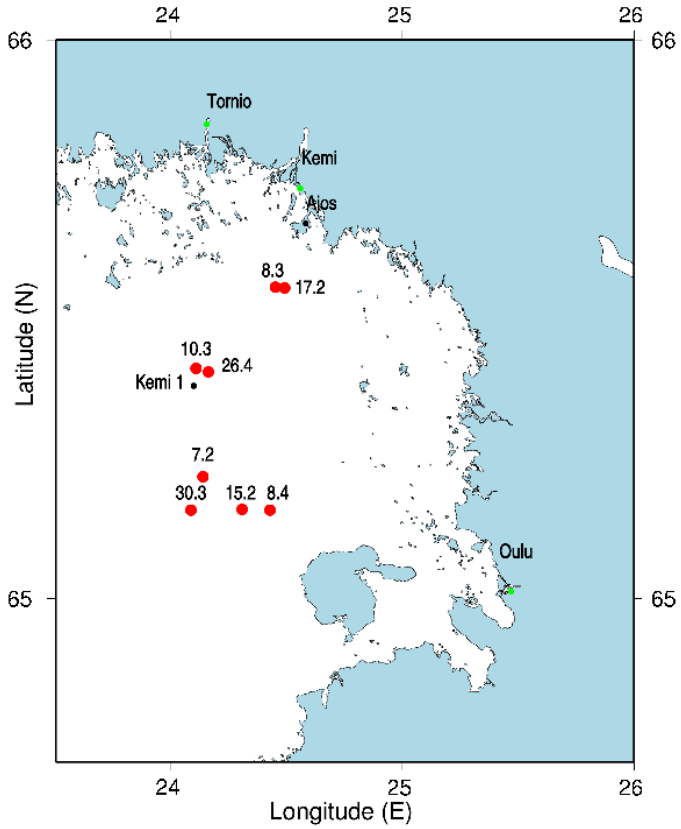

Fig. 21. The location of the identified compression cases.

In the following a selection of the identified compression cases are analyzed. This means that the IceCam images are presented and the possible channel closing speeds are estimated, weather described, ice conditions described, ship route and speed along the route described and for one case the compression forecasts have been analyzed.

5.2 Case 1, 7th of February

Ship Route

According to the reports of icebreaker Otso, pressure in the ice field occured between Kemi1 and Merikallat (circle in Fig. 22). In addition to the optical images, the IceCam provides ship position and speed data. Maps show the ship track marked with different colors depending on the velocity of the ship. Blue color indicates a slow speed, and a red color high speeds. The seaports are marked with green dots on the map. Weather stations Ajos and Kemi 1 are marked with black points. The black ring shows the regime where I/B Otso has reported on the ice compression. The ice chart (Fig. 23) indicates that there has occurred rafting in a level ice field.

Wind Conditions

Figs. 24 and 25 show the observed wind speed and direction at Kemi 1, starting from 0 UTC on 1.2. until 7.2.2005 23.59 UTC. On February 6th the wind direction has shifted to the south and the wind speed increased significantly. Maximum wind speed was 15 m/s.

Water Level Conditions

Due to the shift of the wind conditions, the water level measurements (Fig. 26) show a rapid rise from February 6th to the evening of February 7th.

Strain calculations from IceCam images

The calculation of strain in the ice sheet indicates pressure in the ice field (Fig. 27).

The IceCam Images

The picture analysis is based on the original IceCam pictures taken on board the ship. These pictures have been selected by going though all the pictures taken during the reported events. The images from this case are shown in Fig. 28.

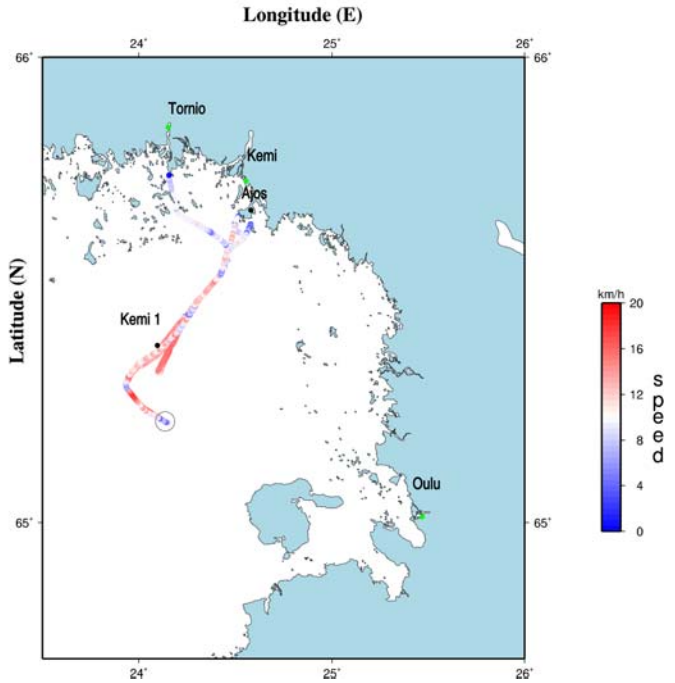

Fig. 22. Route of the I/B Otso on 7.2.2006. The color indicates the speed of the ship (km/h).

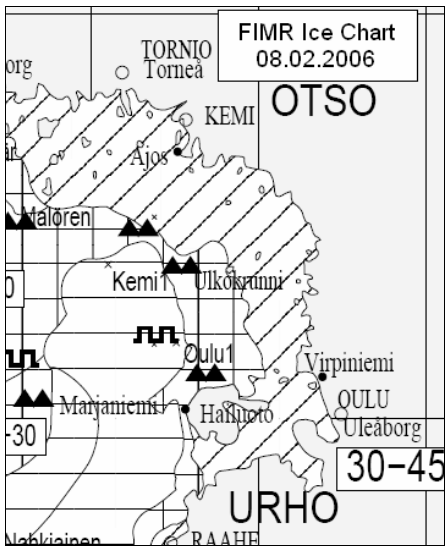

Fig. 23. FIMR Ice Chart from 8.2.2006.

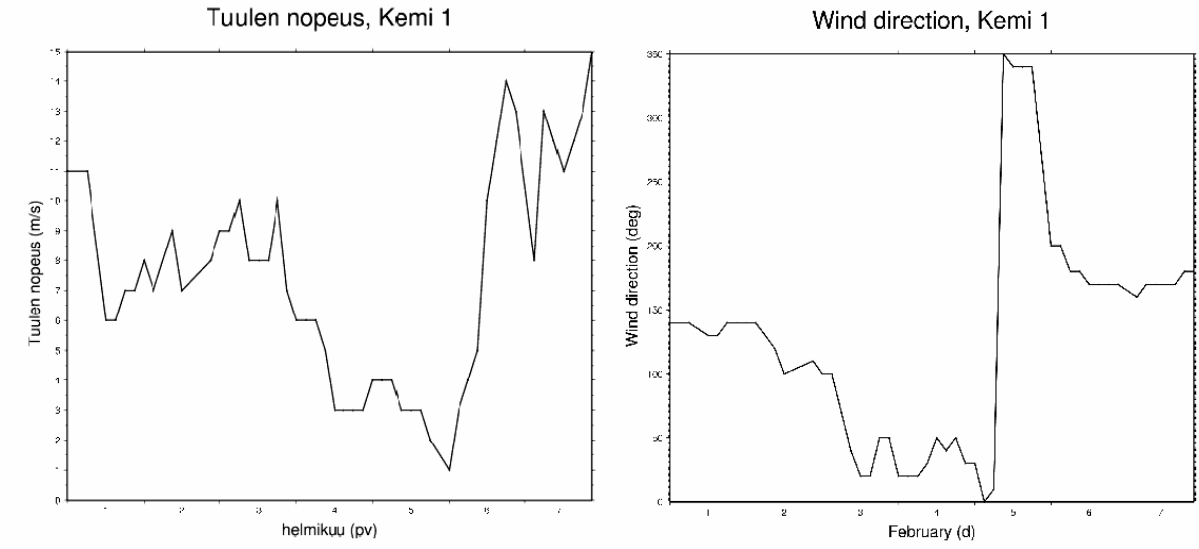

Figs. 24 and 25. Wind speed and direction at Kemi1, 1.-7.2.2006.

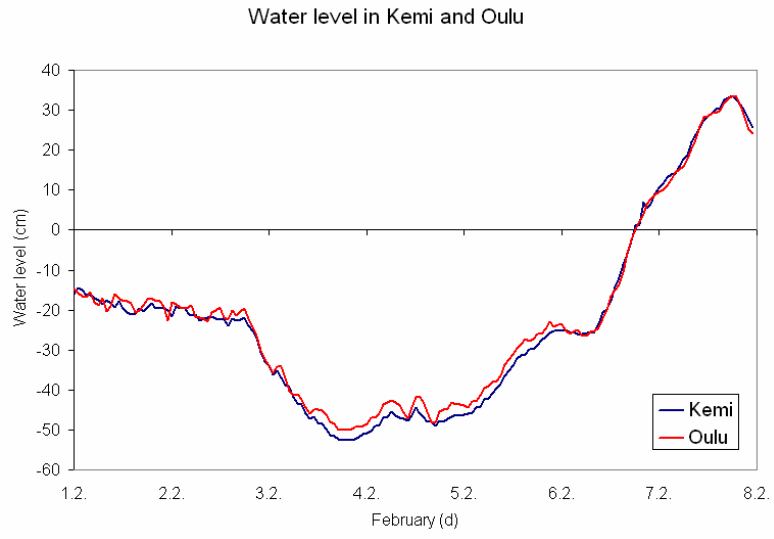

Fig. 26. Water levels in Kemi and Oulu 1.-7.2.2006.

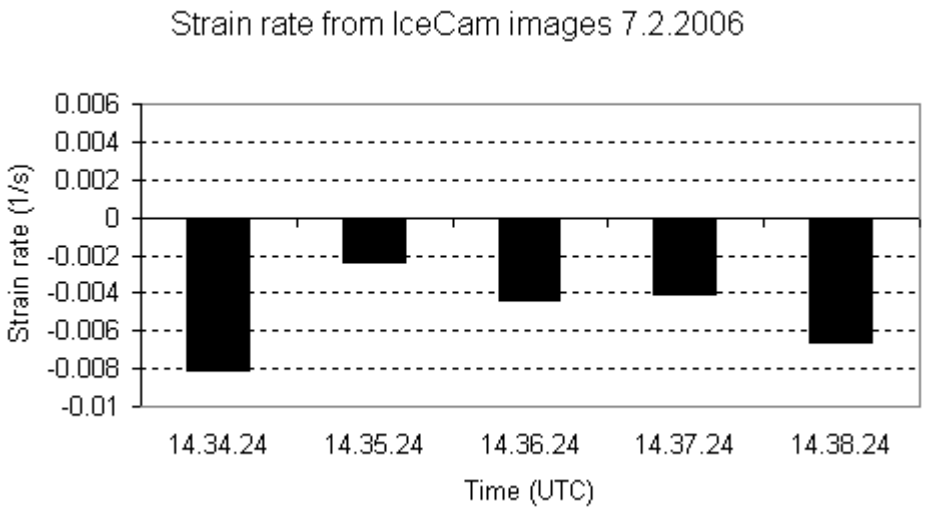

Fig. 27. Strain rate calculations from IceCam images. Ship course in all images 122-123 degrees.

Fig. 28a. Date: 07.02.2006 time: 14:35.

Fig. 28b. Date: 07.02.2006 time: 14:37.

5.3 Case 2, 15th of February

Ship Route

According to the reports of I/B Otso, pressure in the ice field occured off Oulu1 (circle in Fig. 29). The ice chart (Fig. 30) indicates that there has occurred rafting in a relatively thick level ice field.

Wind Conditions

The observed wind speed and direction at Kemi 1, starting from 0 UTC on 11.2. until 17.2.2005 23.59 UTC (see fig.32 in Case 3) shows an increase in wind speed on February 15th. Maximum wind speed was 14 m/s. The wind direction stays in a stable fashion in southerly values (Fig.36 in Case 3).

Water Level Conditions

Also the water level measurements show a rapid rise during February 15th (Fig.38 in Case 3).

Strain calculations from IceCam images

The calculation of strain in the ice sheet indicates a stable pressure in the ice field (Fig. 31).

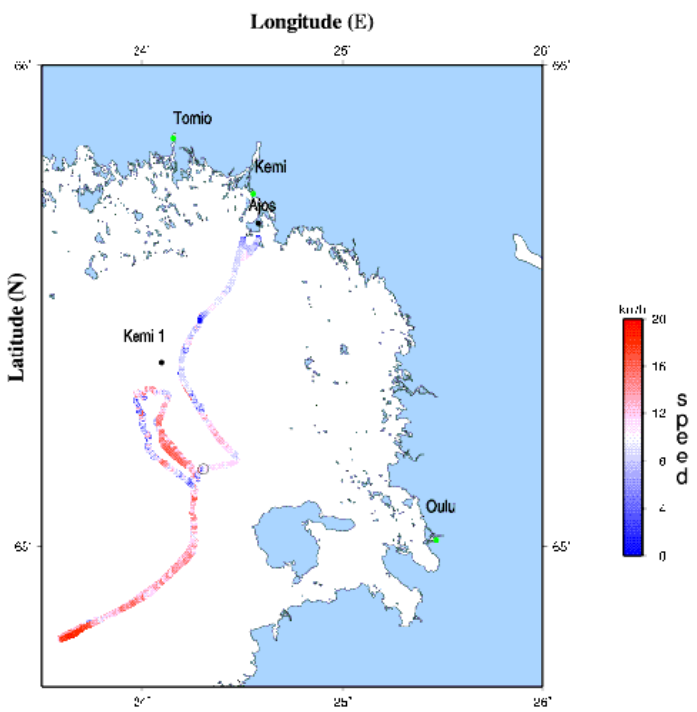

Fig. 29. Route of the I/B Otso on 17.2.2006. The color indicates the speed of the ship (km/h).

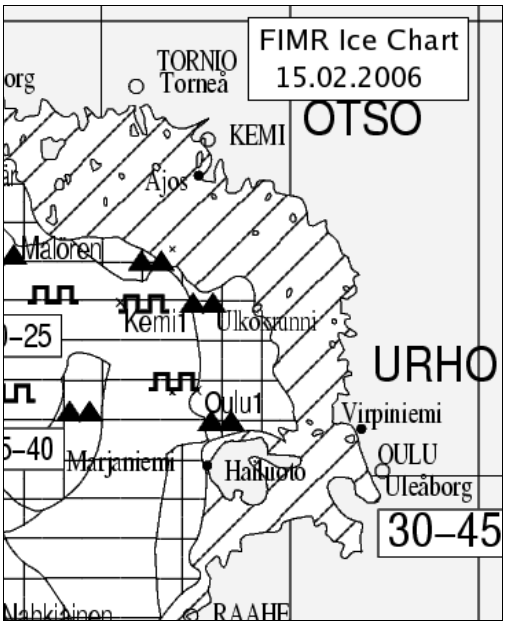

Fig. 30. FIMR Ice Chart from 15.2.2006.

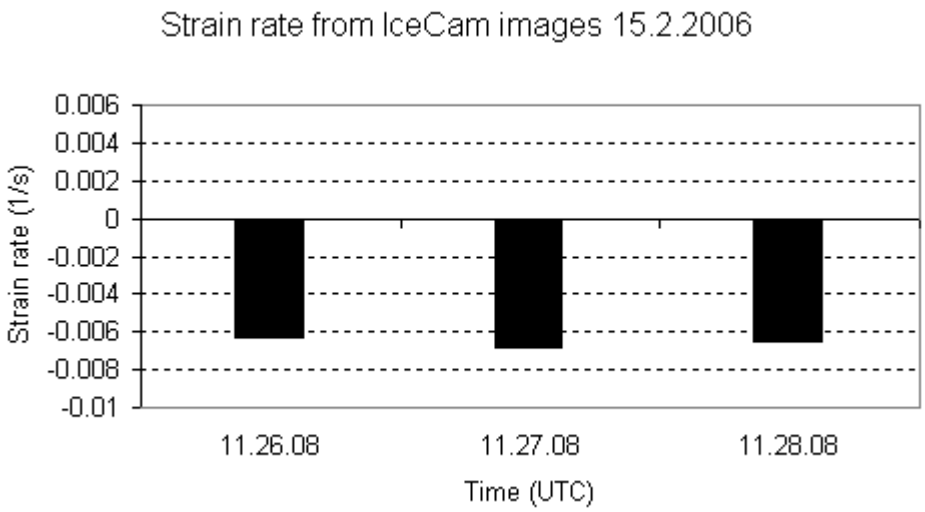

Fig. 31. Strain rate calculations from IceCam images. Ship's course in all images 133 degrees.

Fig. 32. Date: 15.02.2006 time: 11:28.

5.4 Case 3, 16th and 17th of February

Ship Route

According to the reports of I/B Otso ice pack has moved and the channels were closing on 16th and 17th of February in the Botnian Bay. The IceCam data from 16th of February is unfortunately not usable because of the trail of a ship. This analysis is concentrated on the 17th of February route (Fig. 33). The ice chart (Fig. 34) shows a thicker floe of ridged ice that has drifted to the area.

Wind Conditions

Figures 35 and 36 show the observed wind speed and direction in Kemi 1 on 17 February. Starting from 0 UTC on 16.2. till 17.2.2005 23.59 UTC. The wind direction has been mostly from the south, south-east, and the wind speed has been moderate. Maximum wind speed was 12 m/s.

Water Level Conditions

The water level measurements show a quite rapid decline during February 16th and 17th (fig.37).

The IceCam Images

The pictures below (Figs. 38 and 39) show the compression in the ice as it was detected by the icebreaker crew; the previous channel was closed. In the images the ship is heading to north-west and the wind direction is from south, south-east. The channel the icebreaker makes at the moment the images were taken, no compression evidenced by channel closing is detected.

In figure 33. the ship's coordinates are 65º 33.4960' N 24º 29.7076' E. The picture has been taken in the assumed compression region. The ice field seems very stable, and the channel stays straight after the ship. In the image 36. the ship's coordinates are 65º 33.6036' N 24º 29.3587' E, which is taken one minute after the image 38. From this image disturbance in the ice field is detected. The ice has suddenly moved and a curve in the channel has formed. To analyze more of this picture the corrected pictures are used.

The first corrected picture (Fig. 40) is presenting the situation before the formed curve. The channel is straight and very easily identified. In the second picture (Fig. 41) a curve is formed, but not any clear trace of pressure is noticed. The channel stays quite stable and open.

Conclusion

The captain's report from the ship tells about closing channels between Välikivikko and Kemi 1, which are located close to Ajos. The study area is situated between these two places.

There is no clear trace of pressure in the study area. The curve in the channel is recogniced, but after this bent the channels are not closing. It is possible that there has been a ridge which has been hard to drive though. It is also possible that there is pressure, but the pressure is not perpendicular to the ship. The wind direction is also more from behind the ship.

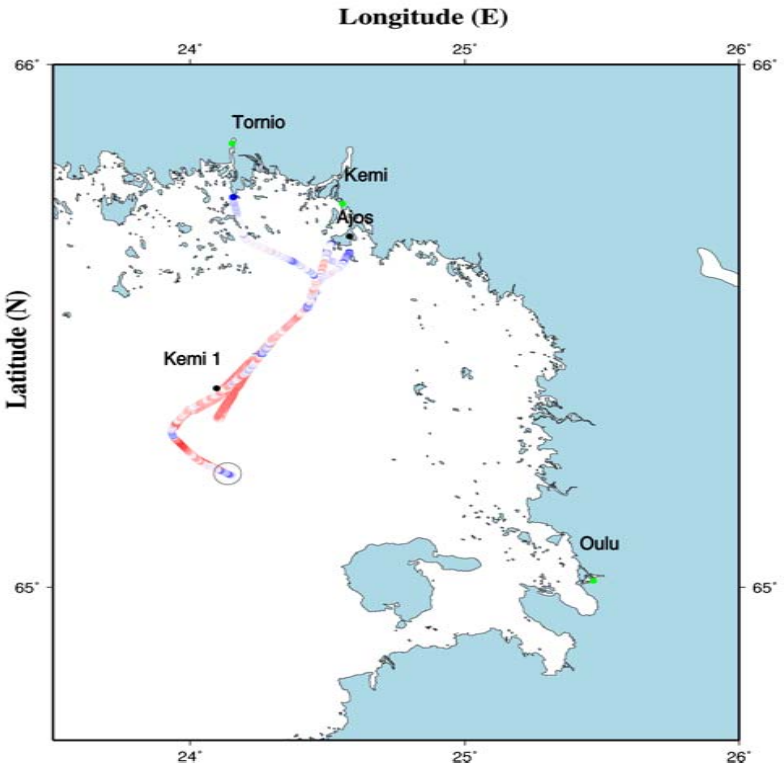

Fig. 33. Route of the I/B Otso on 17.2.2006. The color indicates the speed of the ship (km/h).

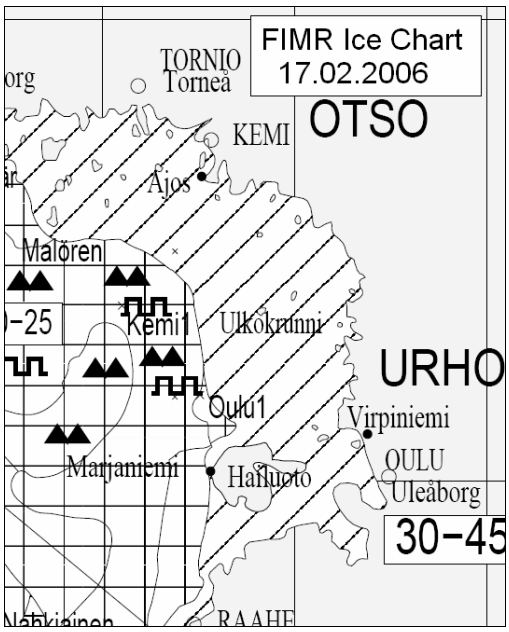

Fig. 34. FIMR Ice Chart from 17.2.2006.

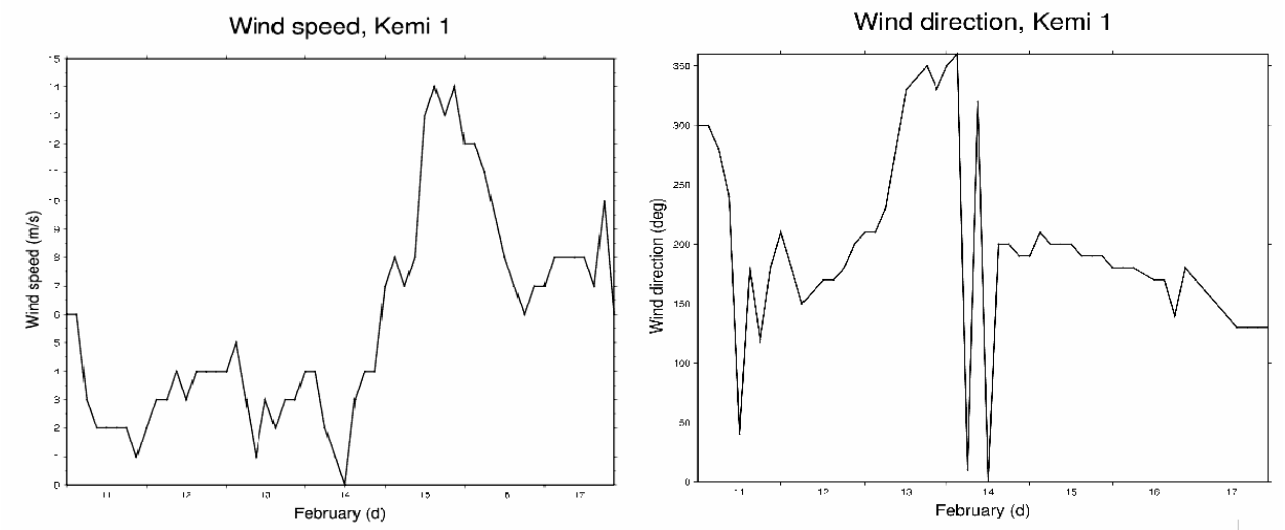

Figs. 35 and 36. Wind speed and direction at Kemi1, 11.-17.2.2006.

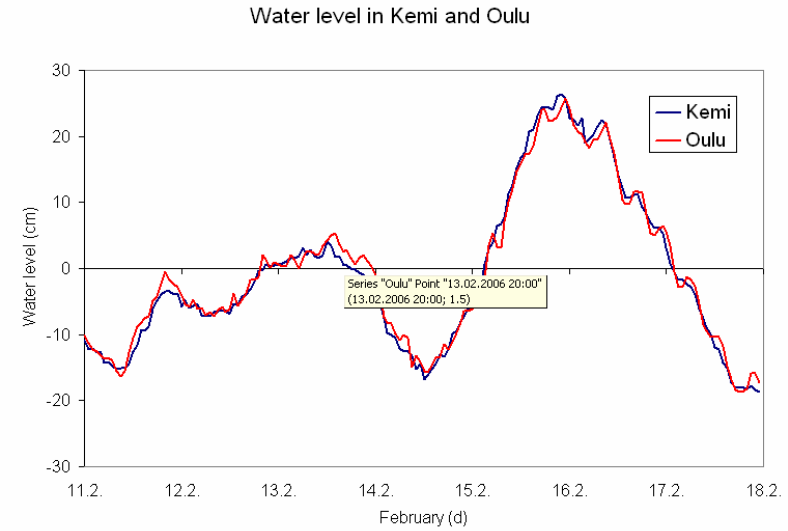

Fig. 37. Water levels in Kemi and Oulu 11.-17.2.2006.

Fig. 38. Date: 17.2.2005 time: 15.32.40.

Fig. 39. Date: 17.2.2005 time: 15.33.40.

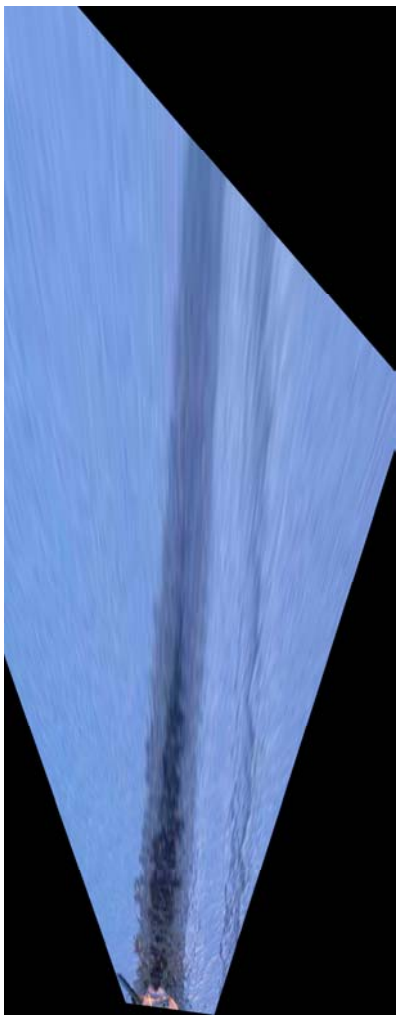

Fig. 40. Corrected image 17.2.2005 time:15.32.40

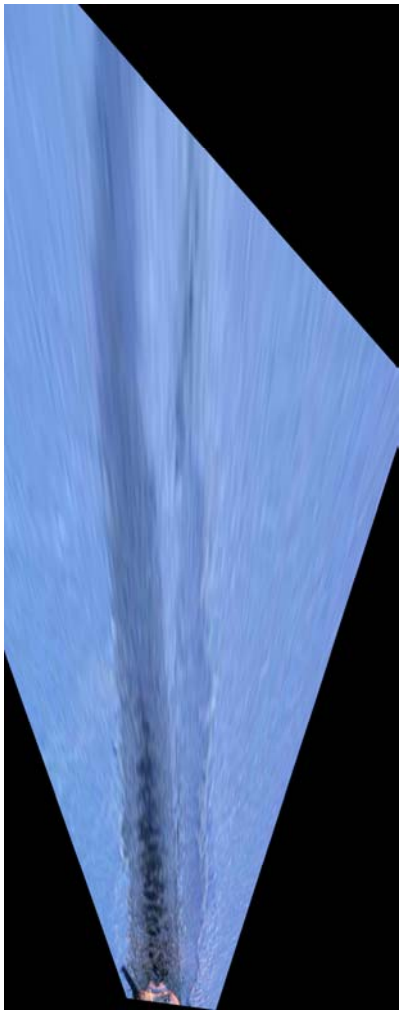

Fig. 41. Corrected image 17.2.2005 time: 15.33.40

5.5 Case 4, 8th of March

Ship Route

The I/B Otso reports pressure in the ice field west-northwest of Merikallat (circle in Fig. 42). The ice chart (Fig. 43) shows a level ice field in that area.

Wind Conditions

The observed wind speed and direction at Kemi 1, starting from 0 UTC on 2.3. until 8.3.2005 23.59 UTC (Fig. 44) shows very low wind speeds during the last two days. Maximum wind speed on March 8th was 4 m/s. The wind directions during the last two days are mainly northerly (Fig. 45).

Water Level Conditions

Water level measurements show only a slow rise during the period (Fig. 46). The water level is quite low, however.

Strain calculations from IceCam images

No strain calculations are done due to sea smoke and assistance of vessels.

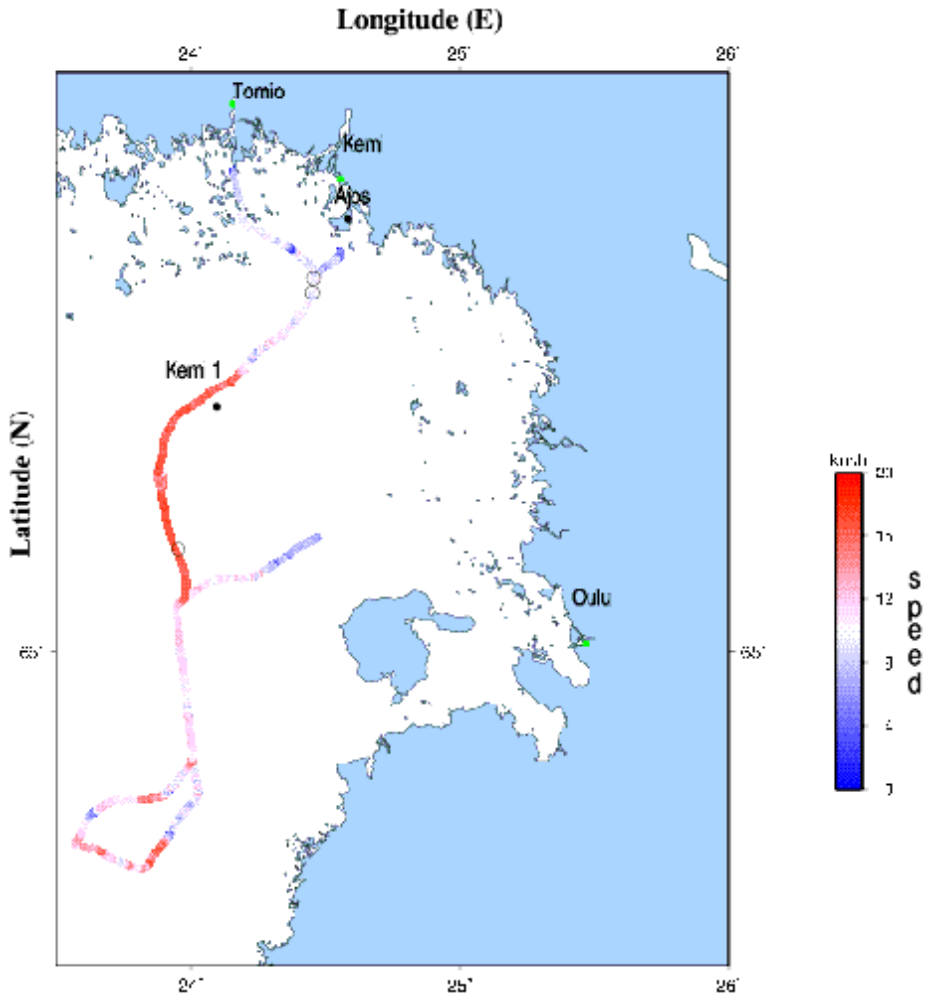

Fig. 42. Route of the I/B Otso on 08.03.2006. The color indicates the speed of the ship (km/h).

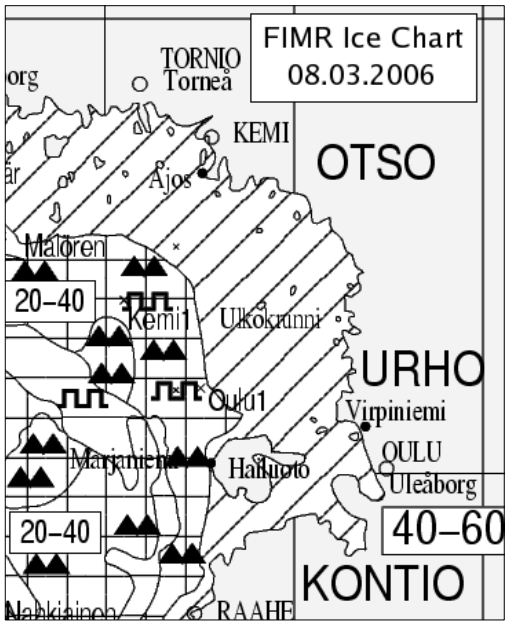

Fig. 43. FIMR Ice Chart from 8.3.2006.

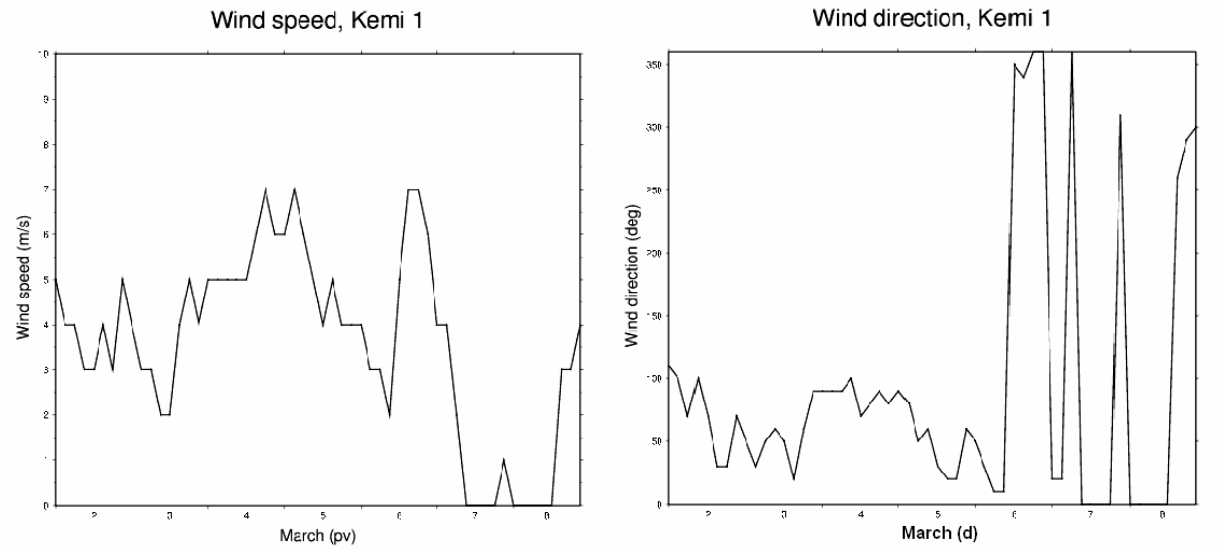

Figs. 44 and 45. Wind speed and direction at Kemi1, 2.-8.3.2006.

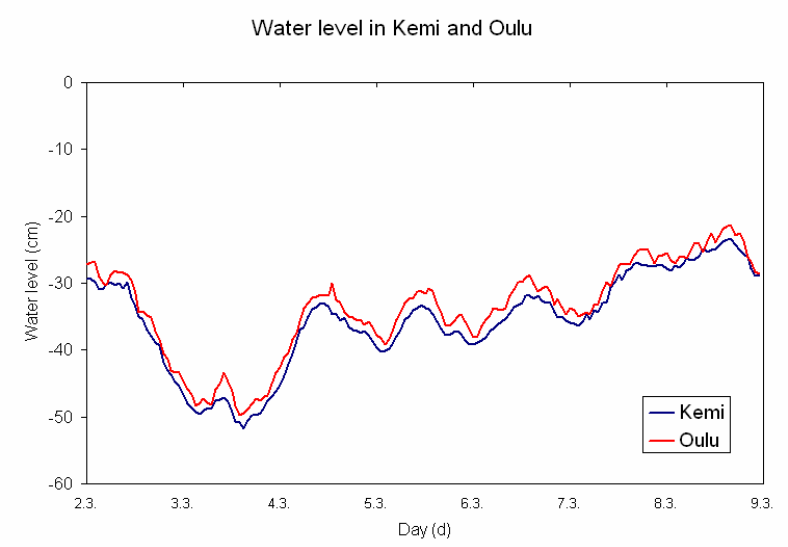

Fig. 46. Water levels in Kemi and Oulu 2.-8.3.2006.

Fig. 47. Date: 08.03.2006 time: 10:34.

5.6 Case 7, 8th of April

Ship Route

According to the reports of I/B Otso the drifting ice pack caused ice pressure when it was pressed against the fast ice edge along the fairway south-east of the lighthouse Oulu 1 (Fig. 48). The ice chart of that day shows a large ridged ice floe north-west of Hailuoto island that streches to light house Oulu1 (Fig. 49). The forecasted ice pressure (Fig. 50) shows a small point-like area with pressure in the vicinity of Oulu1.

Wind Conditions

Figs. 51 and 52 show the observed wind speed and direction at Kemi 1 on 8 April, starting from 0 UTC on 2.4. until 8.4.2005 23.59 UTC. The wind direction has during the three last days been mostly from the south-east, and the wind speed has been only moderate. Maximum wind speed was 14 m/s.

Water Level Conditions

The water level clearly has responded to the changed wind direction on April 6th by rising over the zero level. During saturday 8th of April a further rising in the water level is observed (Fig. 53).

Strain calculations from IceCam images

The calculation of strain in the ice sheet indicates both negative and positive pressure in the ice field (Fig. 54).

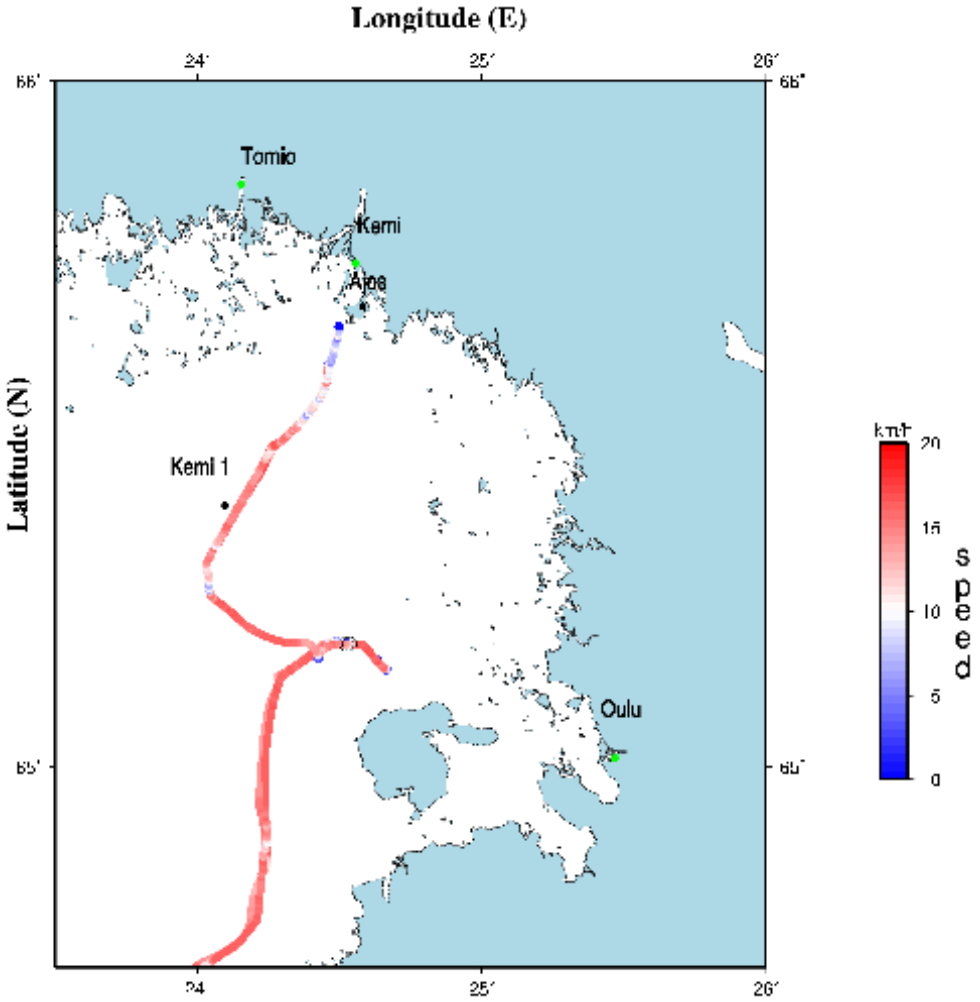

Fig. 48. Route of the I/B Otso on 08.04.2006. The color indicates the speed of the ship (km/h).

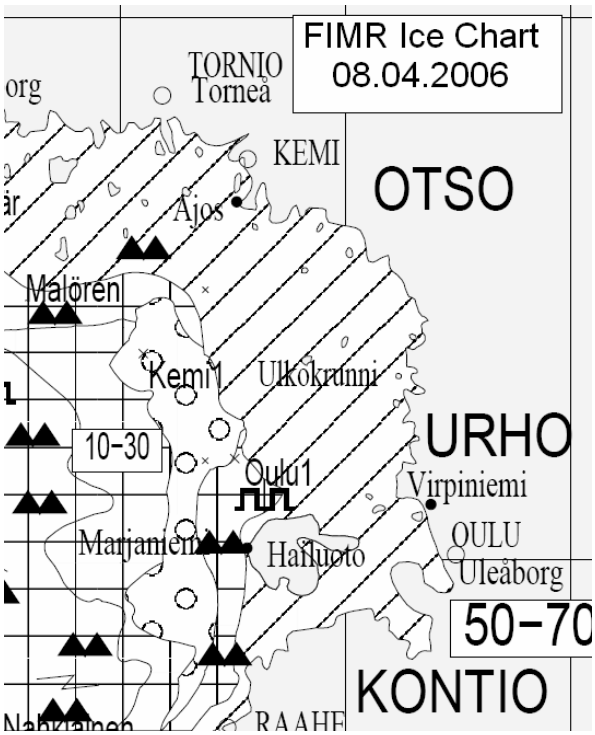

Fig. 49. FIMR Ice Chart from 8.4.2006.

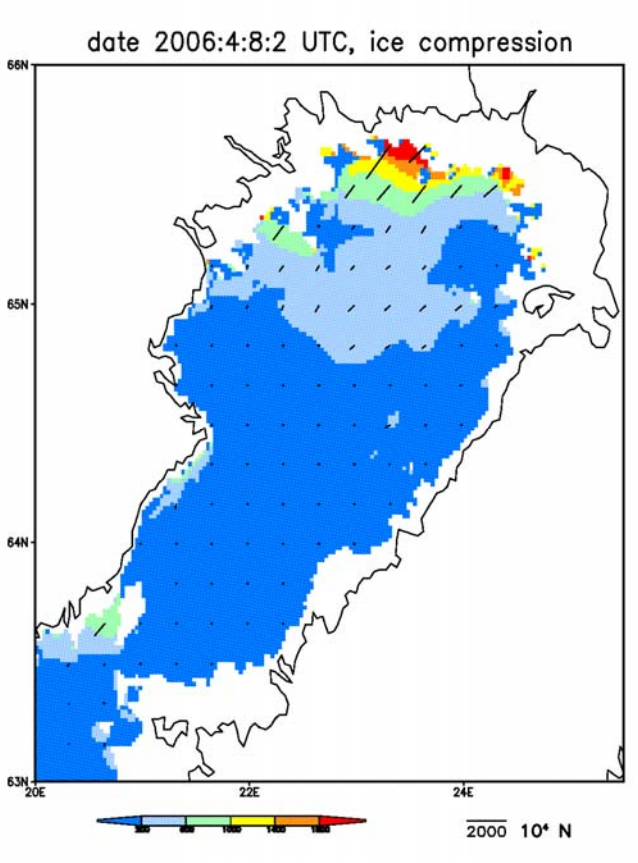

Fig. 50. Forecasted ice pressure for 8.4.2006.

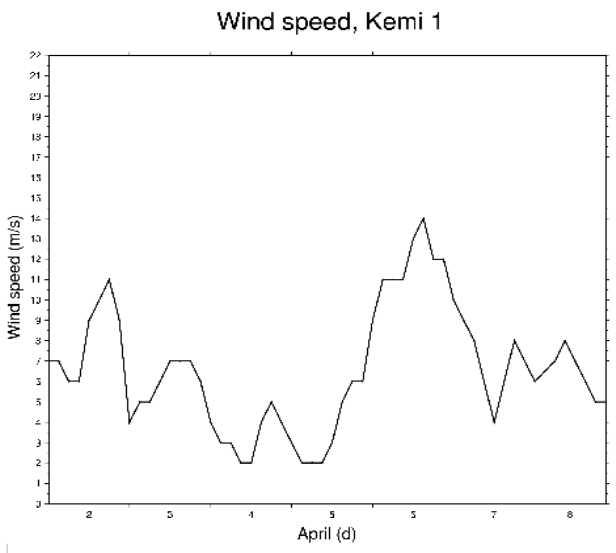

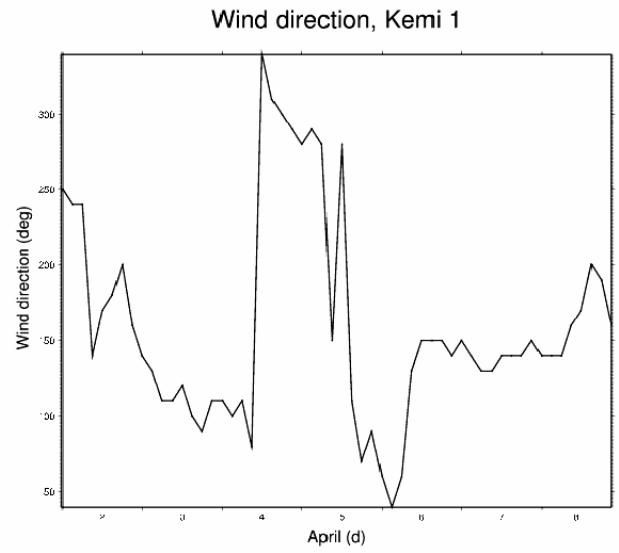

Figs. 51 and 52. Wind speed and direction at Kemi1, 2.-8.4.2006.

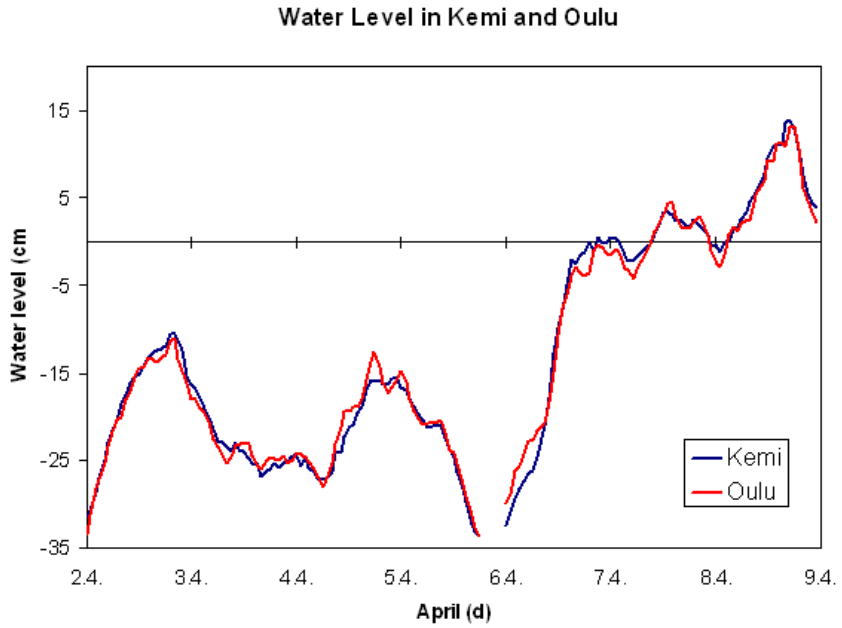

Fig. 53. Water levels in Kemi and Oulu 2.-8.4.2006.

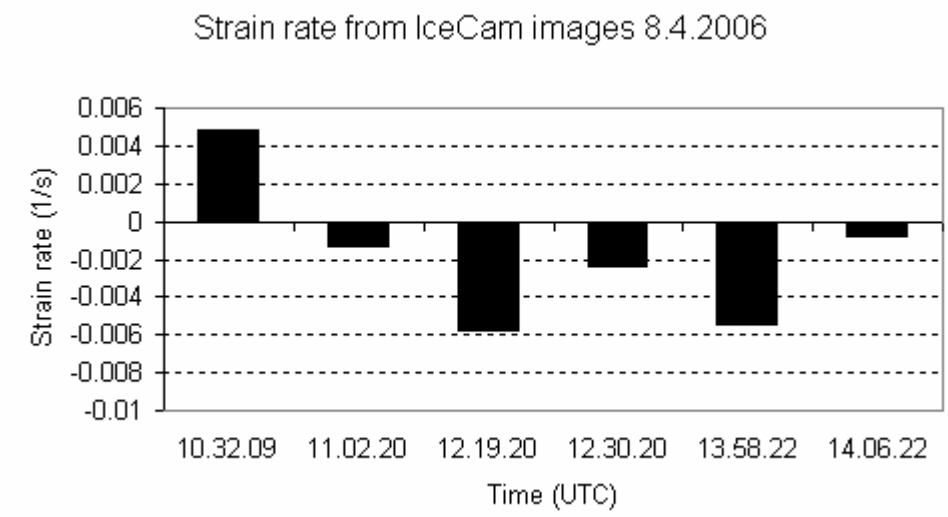

Fig. 54. Strain rate calculations from IceCam images.

Fig. 55. Date: 08.04.2006 time: 10:32.

Fig. 56. Date: 08.04.2006 time: 13:58.

5.7 Application of Analyzed Cases on Navigation in Compressive Ice

One of the targets of this research project was to develop a measure for compression that can be used in ship routing. This has been discussed earlier in the context of modeling the ice cover. Here the experience from the observed compressive cases is used to make some general comments on navigation in compressive ice cover.

Direction

The stresses in ice can be used to determine the principal stresses. It is usually assumed that the larger principal stress is dominating and this means that the compression has I direction. This conclusion is supported by the observation of closing ship tracks after the vessels. If the ship is moving along the main direction of compression (i.e. in the direction of larger principal stress), the ship track is not necessarily closing after the vessel. This suggests the importance in selecting the route through compressive ice.

The direction to minimize the effects of compression – once the direction is known – was suggested above. If the ice field is not moving, it is not easy to know the principal stress direction. The wind direction gives an indication, but only an indication. As the compression forms under driving forces and a boundary against which the ice is pushed, it can be inferred that the compression is large towards the coastline. Thus the compression is felt most strongly when proceeding along the coastline. This description of compression indicates also that the compression will cease inside the archipelago.

As noted earlier, the ice motion is somewhat right from the wind direction because of the Coriolis effect. The stress direction and ice drift direction is not the same and it is more generally the case that ice drift and ice compression are different things.

Onset of ice motion

At least one case was observed with the IceCam where the ship passage triggered the onset of ice motion. In this case the ship track did not only close after the vessel but the field started moving. This was probably because the inertia that the ice cover collected when it started moving, made it overcome the resistance for compressing the field given by rafting and/or ridging forces. This type of onset of ice motion due to ship passage should be avoided for example in locations where two ice floes are pressing against each other, see Fig. 57. If the vessel is to pass through the contact point, the ship passage could trigger motion of the floes and the ship would get stuck between two floes. The passage through the other floe is to be preferred.

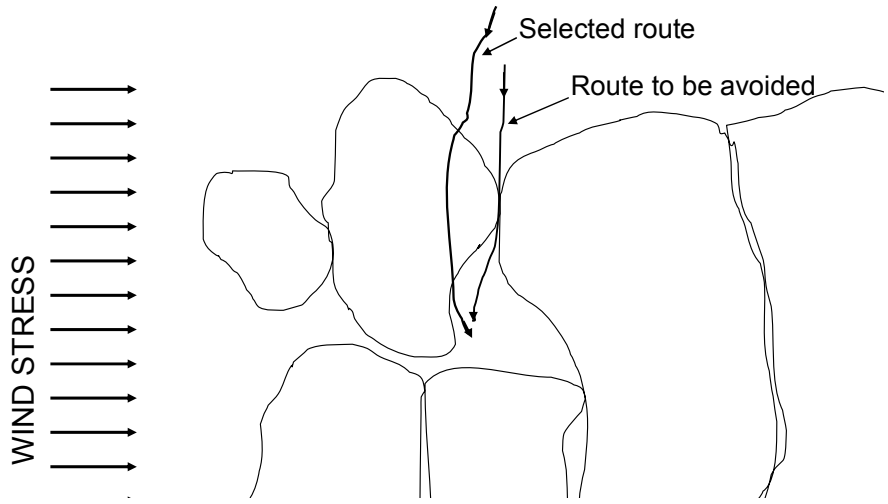

Fig. 57. The route selection at the contact of two large ice floes.

Duration of compression

The observed and also forecasted situation where there was compression in the ice cover lasted relatively short time, some hours. The compression changed and usually eased when the wind direction changed or the wind velocity decreased. The wind velocity did not stay high and from the same direction long time. Thus it can be concluded that firstly, if the ship is in a compressive ice field, the situation remains the same as long as the wind speed remains high AND the wind direction does not change. The situation will change rapidly when either wind characteristic changes.

6 OPERATIVE FORECASTING OF COMPRESSION

Within the ice pressure prediction project, the Ice Service at FIMR composed ice pressure forecasts during the first winter of activity. The on-duty scientist made three test forecasts during the winter. They were dated 23.2. 15.3. and 17.3.2006. These forecasts were sent to the Finnish icebreakers operating in the Northern Baltic Sea. The forecasts all concerned the Bay of Bothnia. Ice pressure model calculations were also made for the Gulf of Finland but no such occasion appeared where it would have made sense to compose a forecast.

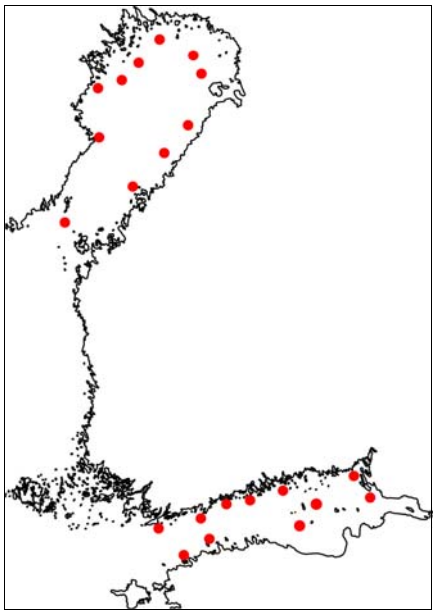

Fig. 57: The points for calculation of the time series with the ice pressure model.

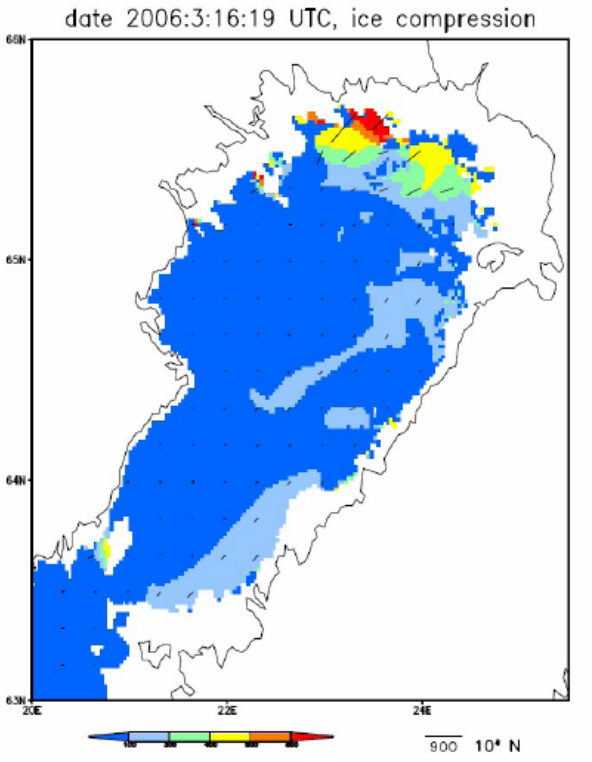

Fig 58: Map of ice pressure distribution.

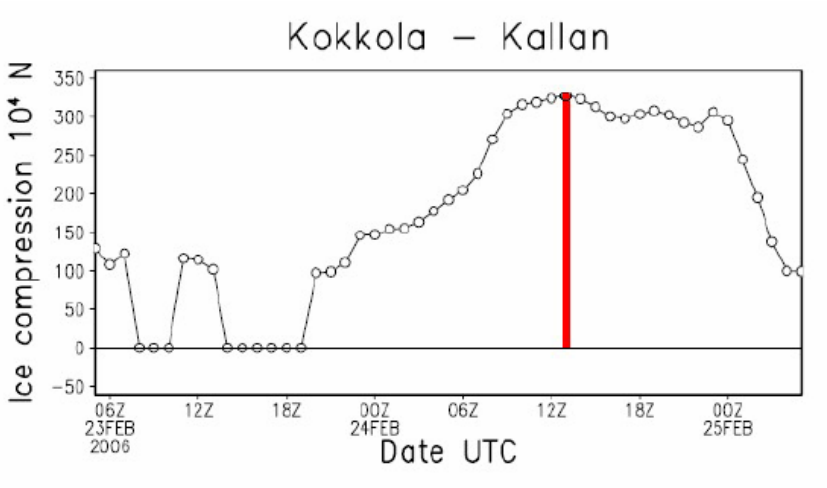

Fig. 59: Time series of ice pressure magnitude at Kallan.

Composing the forecasts

The ice pressure forecasted by the ice model was printed as time series from eleven positions in the Bay of Bothnia and eleven positions in the Gulf of Finland (map, appendix 6.1). Maps showing the ice pressure magnitude and direction were also printed, two for each sea area. These were chosen for times when maximum pressure occurred. The colour scale in the forecast maps indicates the pressure magnitude according to the power scale in the legend bar. The lines on the maps show a direction for the ice pressure so that the pressure is strongest in the direction indicated. The time series show the model predicted ice pressure for one position. The span of the time series is 48 hours.

When composing the forecasts, the above mentioned ice model runs were available at the Ice Service every day at 11 am. As the forecasts were made during the afternoon they reached about 38- 40 hours forward in time.

For the forecasts the graphs with most relevance were picked from the model printouts. For example in the forecast # 1 (23.02.2006) two time series were chosen where the time of ice pressure maxima differed from each other. The maps showed the ice pressure distribution in the Bay of Bothnia for the corresponding times. A red bar was added into the time series to pinpoint the time of occurrence for the maximum pressure, see Fig. 57. For the forecast # 3 only one map was chosen with time series for three separate positions. This because the time of maximum pressure coincided for the whole Bay of Bothnia.

Also a text of the predicted ice pressure was included in the forecast. The written section contained information about the time, location and the magnitude of the ice pressure, as well as in which direction it is easiest to navigate. This direction is assumed to be the same in which the pressure force is strongest. In other words, if a vessel moves in this direction the strongest pressure forces are directed towards the bow and the aft of the ship. The direction of easiest motion in this way coincides with the lines in the pressure maps.

At the end of the forecast sheets there was left some space for comments from the user. However, during the spring the Ice Service received no feedback about the forecasts.

Format and delivery of the forecasts

The forecasts were kept single paged in order to keep them consistent. These were saved in PDF format and sent as e-mail attachments to the icebreakers, as well as to director Atso Uusiaho (Finstaship) and the Winter Navigation Department at the Finnish Maritime Administration. An example of these forecasts sent to icebreakers is given in Fig. 60.

Merentutkimuslaitos, Jääpalvelu ice@fimr.fi **puhelin (09) 685 7659**

Jäänpuristusennuste Perämerelle No 3/2006 17.3.2006

18.3. klo 14:00

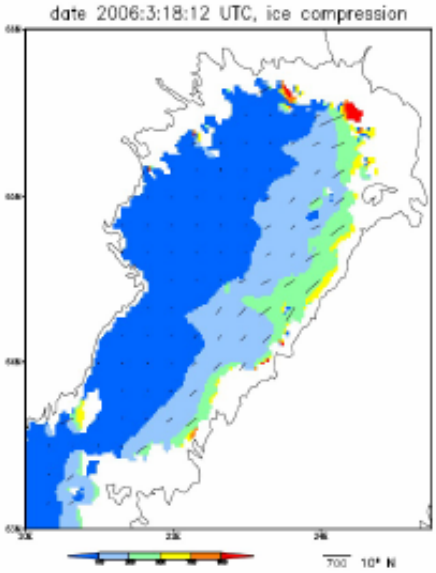

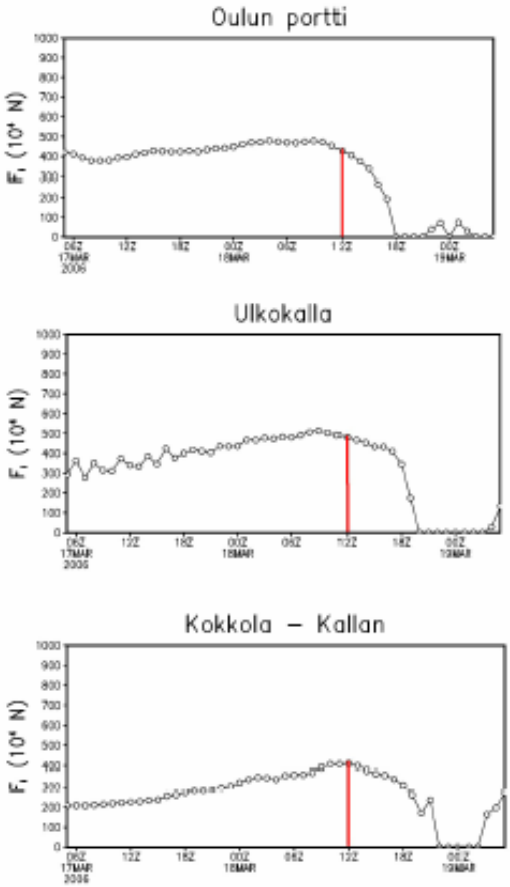

Perämeri: Lauantaina 18.3. Suomen rannikon edustalla on odotettavissa heikkoa puristusta. Helpoimman liikkumisen suunta on noin 45°-225°. Puristus lakkaa iltaan mennessä tuulten kääntyessä.

Arvio ennusteen paikkansapitävyydestä:

	Piti paikkansa hyvin/huonosti/jotenkin	Miten poikkesi havaitusta? voimakkuus	Miten poikkesi havaitusta? suunta	Muuta
P. Perämeri				
Kesk. Perämeri				
Muu alue/paikka:				

Vapaat kommentit:

pe

Ennuste perustuu vallitsevaan jäätilanteeseen ja sääennusteisiin.

Fig. 60. The draft of the ice compression forecasts sent to icebreakers for comments.

7 SUMMARY AND SUGGESTIONS FOR FUTURE WORK

The operative forecasting of compression in ice is a new topic for research and development. Most ice charts issued by various ice services try to predict the occurrence of compression but so far no quantitative measures for compression have been presented. Mostly the compression is at present identified by the presence of driving forces and a boundary i.e. driving force (wind or current drag) acting towards the shoreline.

In the present report the results from a project to develop a measure for the compression in an ice cover that would be suitable for shipping – and also delivered to shipping in an operative manner suitable for navigation guidance – are described. The research work included investigation of the action of compressive ice on ships, development of ice dynamics forecasting models, observation of compression onboard an icebreaker and delivery of forecasts to icebreakers. As the development of a suitable measure for compression proved to be difficult, the images of ship channel taken onboard the icebreaker Otso were analyzed in order to gain an insight what is the proper or at least adequate measure for compression. The cases when IB Otso observed compression were also analyzed in order to make some conclusion about navigation in a compressive ice field.

The adequate measure for compression was identified in the project. As the measure (load on horizontal unit distance) in the ice cover is from dynamic ice modeling, this has to be down-scaled in order to be useful in ship-scale. A suggestion for this was made, but more research is needed, especially to clarify the influence of ship course versus the direction of the principal stress in ice. This work to investigate the effect of compression on ships is just the beginning and should be continued with getting more data about compressive situations.

Forecasts of ice compression were made during the winter 2006 and delivered to selected icebreakers. The feedback from the forecasts was collected in form of icebreaker crew comments stated in the IBNet system. Several cases of compression was identified and analyzed in detail. In general the icebreakers observed compression at the same time and same area as the forecasts predicted compression. A thorough analysis of the described cases should be carried out.

The visual appearance of the forecasts is not final and may well change during the coming seasons. In this sense we still gladly accept any feedback about the layout, format and content of the forecast from icebreaker operators and other users.

The color scale of the forecast maps will be improved so that the ice covered areas appear more clearly. Open water and fast ice will also be clearly distinguished. When composing the forecasts, certain work steps have to be carried out automatically. This way the work will occupy less time beside other operational tasks. The aim is to run the ice model later than last winter so that the prediction range will stretch further in time. Example: Model is run with the 12 AM weather, being ready around 3 PM and reaching thus 45 hours forward.

A considerable improvement would be gained using a longer time scale for the ice forecasting model. This is, however, dependent on the length and accuracy of the weather forecasts.

REFERENCES

Flato, G. M. & Hibler III, W.D. 1995. Ridging and Strength in modeling the thickness distribution of Arctic Sea Ice, Journal of Geophysical Research 100:18611-18626.

Haapala, J. & Lönnroth. N. and Stössel, A. (2005). A numerical study of open water formation in sea ice, J.Geophys.Res.110, C09011, doi: 10.1029/2003JC002200

Hall, R.J. & Hughes, N.E. and Wadhams, P. (2002). A systematic method of obtaining ice concentration measurements from ship-based observations. Cold Regions Science and Technology, 34(2), pp. 97-102.

IceCam homepage: http://www.nersc.no/ICEMON/icecam.php.

Kujala, P. 1991: Damage Statistics of Ice-Strengthened Ships in the Baltic Sea. Winter Navigation Research Board, Research Report No. 50, Helsinki.

Leppäranta, M. 1981: On the Structure and Mechanics of Pack Ice in the Bothnian Bay. Finnish Marine Research, 248, 86 p.

Riska, K. & Breivik, K. & Eide, S.I. & Gudmestad, O. and Hilden, T. 2006: Factors Influencing the Development of Routes for Regular Oil Transport from Dikson. Proc. ICETECH06, Banff, Canada, July 16-19, 2006, Paper 153.

Rothrock, D.A. 1975: The Energetics of the Plastic Deformation of Pack Ice by Ridging. Journal of Geophysical Research, Vol. 80, No. 33, pp. 4514 – 4519.

Zubov, L'dy Arktiki [Arctic Ice]. Izdatel'stvo Glavsevmorputi, Moscow [English translation 1963 by US Naval Oceanological Office and American Meteorological Society, San Diego, 490 p.].

APPENDIX Points for calculation of time series with the ice pressure model.

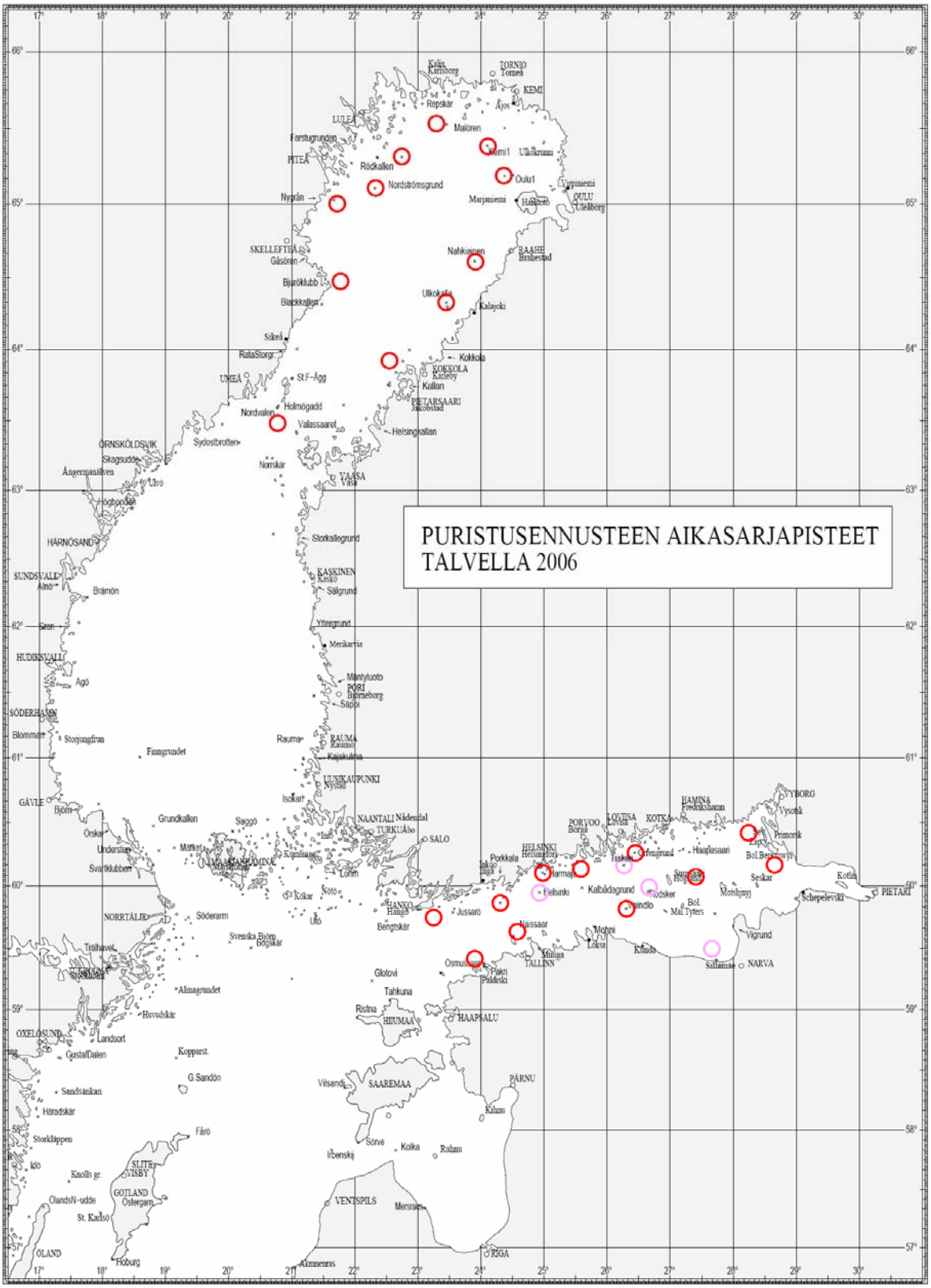

Edita Prima Oy
ISBN 978-951-49-2152-0
ISSN 0348-9485